



# Silicon Isotopes Reveal a Non-glacial Source of Silicon to Crescent Stream, McMurdo Dry Valleys, Antarctica

Catherine Hirst<sup>1\*</sup>, Sophie Opfergelt<sup>1</sup>, François Gaspard<sup>1</sup>, Katharine R. Hendry<sup>2</sup>, Jade E. Hatton<sup>2</sup>, Susan Welch<sup>3</sup>, Diane M. McKnight<sup>4</sup> and W. Berry Lyons<sup>3</sup>

<sup>1</sup> Earth and Life Institute, Environmental Sciences, Université catholique de Louvain, Louvain-la-Neuve, Belgium, <sup>2</sup> School of Earth Sciences, University of Bristol, Bristol, United Kingdom, <sup>3</sup> School of Earth Sciences, Byrd Polar and Climate Research Center, The Ohio State University, Columbus, OH, United States, <sup>4</sup> Institute of Arctic and Alpine Research, University of Colorado Boulder, Boulder, CO, United States

## OPEN ACCESS

### Edited by:

Andrew Jonathan Hodson,  
The University Centre in Svalbard,  
Norway

### Reviewed by:

Yigal Erel,  
Hebrew University of Jerusalem, Israel  
Martin Guitreau,  
Université Clermont Auvergne, France

### \*Correspondence:

Catherine Hirst  
catherine.hirst@uclouvain.be

### Specialty section:

This article was submitted to  
Geochemistry,  
a section of the journal  
Frontiers in Earth Science

**Received:** 09 March 2020

**Accepted:** 28 May 2020

**Published:** 26 June 2020

### Citation:

Hirst C, Opfergelt S, Gaspard F, Hendry KR, Hatton JE, Welch S, McKnight DM and Berry Lyons W (2020) Silicon Isotopes Reveal a Non-glacial Source of Silicon to Crescent Stream, McMurdo Dry Valleys, Antarctica. *Front. Earth Sci.* 8:229. doi: 10.3389/feart.2020.00229

In high latitude environments, silicon is supplied to river waters by both glacial and non-glacial chemical weathering. The signal of these two end-members is often obscured by biological uptake and/or groundwater input in the river catchment. McMurdo Dry Valleys streams in Antarctica have no deep groundwater input, no connectivity between streams and no surface vegetation cover, and thus provide a simplified system for us to constrain the supply of dissolved silicon (DSi) to rivers from chemical weathering in a glacial environment. Here we report dissolved Si concentrations, germanium/silicon ratios (Ge/Si) and silicon isotope compositions ( $\delta^{30}\text{Si}_{\text{DSi}}$ ) in Crescent Stream, McMurdo Dry Valleys for samples collected between December and February in the 2014–2015, 2015–2016, and 2016–2017 austral seasons. The  $\delta^{30}\text{Si}_{\text{DSi}}$  compositions and DSi concentrations are higher than values reported in wet-based glacial meltwaters, and form a narrow cluster within the range of values reported for permafrost dominated Arctic Rivers. High  $\delta^{30}\text{Si}_{\text{DSi}}$  compositions, ranging from +0.90‰ to +1.39‰, are attributed to (i) the precipitation of amorphous silica during freezing of waters in isolated pockets of the hyporheic zone in the winter and the release of Si from unfrozen pockets during meltwater-hyporheic zone exchange in the austral summer, and (ii) additional Si isotope fractionation via long-term Si uptake in clay minerals and seasonal Si uptake into diatoms superimposed on this winter-derived isotope signal. There is no relationship between  $\delta^{30}\text{Si}_{\text{DSi}}$  compositions and DSi concentrations with seasonal and daily discharge, showing that stream waters contain DSi that is in equilibrium with the formation of secondary Si minerals in the hyporheic zone. We show that  $\delta^{30}\text{Si}_{\text{DSi}}$  compositions can be used as tracers of silicate weathering in the hyporheic zone and possible tracers of freeze-thaw conditions in the hyporheic zone. This is important in the context of the ongoing warming in McMurdo Dry Valleys and the supply of more meltwaters to the hyporheic zone of McMurdo Dry Valley streams.

**Keywords:** silicon isotopes, hyporheic zone, permafrost, weathering, Antarctica

## INTRODUCTION

McMurdo Dry Valleys (MDV), the largest ice-free area of Antarctica, is covered in continuous permafrost, with low surface temperatures and low rates of precipitation. Under these polar desert conditions, groundwater and surface soil water reservoirs are absent (Conovitz et al., 1998), and first-order streams and their surrounding hyporheic zones are isolated conduits for supra-glacial meltwater transport and a loci of weathering (Lyons et al., 1998; McKnight et al., 1998, 1999, 2004).

A wealth of evidence using dissolved element concentrations and ratios (Lyons et al., 1998; Nezat et al., 2001), Sr and Li isotope analysis (Lyons et al., 2002; Witherow et al., 2010; Dowling et al., 2013) and mineralogical studies (Gooseff et al., 2002; Maurice et al., 2002) shows that Si is supplied to the streams by weathering of stream sediments with silicate mineral weathering rates an order of magnitude greater than rates in lower latitude, warmer locations (Gooseff et al., 2002). These studies demonstrate that chemical weathering of silicates occurs in MDV streams (Lyons et al., 2002), despite the cold temperatures, lack of precipitation and low abundance of complexing organic material (Burkins et al., 2001), and thereby contribute to the atmospheric CO<sub>2</sub> draw down over geological timescales (Berner and Berner, 1997).

Taylor Valley streams in MDV are characterized by extensive hyporheic zones, which comprise the sediment pore spaces adjacent to and underneath the stream through which stream water exchanges. This zone also is the accommodation space that must be filled before stream flow occurs. Mineral dissolution in the hyporheic zone is the commonly accepted contributor to stream geochemistry (Gooseff et al., 2002), but the model of Gooseff et al. (2002) assumes no precipitation reactions of secondary weathering products, including only the net release of solutes from weathering reactions. Secondary weathering products such as clay minerals may form, but the extent to which this occurs within streams is unknown (Lyons et al., 1998; Gooseff et al., 2002). Considering only the net release of solutes from weathering reactions, and not accounting for the formation of secondary weathering products in the near and extended hyporheic zone in MDV streams may contribute to an underestimation of actual weathering rates in this polar region and associated atmospheric CO<sub>2</sub> consumption.

The hyporheic zones in Antarctic streams include near-stream zones where rapid stream-water exchange occurs within hours to days, and extended hyporheic zones, where stream-water exchange occurs over weeks to months (Gooseff et al., 2003). During the austral summer months (November–February), glacial meltwaters, with low Si concentrations (Lyons et al., 2003) are transported through the near and extended hyporheic zone sediments and rapidly react with mineral surfaces (Gooseff et al., 2002) resulting in DSi concentrations that are in near equilibrium with minerals and independent of flow rates (Wlostowski et al., 2018). The questions arise: (i) is the Si released from weathering within the hyporheic zone transferred to the stream with limited formation of secondary weathering products; and (ii) are the controlling factors of the Si transfer from the hyporheic zone to the stream constant, or do they change through the summer with the changing contribution of waters from the extended

hyporheic zone and near-stream hyporheic zone? To answer these questions we use dissolved silicon isotope composition ( $\delta^{30}\text{Si}_{\text{DSi}}$ ) and the germanium/silicon ratios (Ge/Si) to pull apart primary silicate weathering processes, biotic processes and abiotic secondary weathering processes in a permafrost-dominated stream in Antarctica.

The  $\delta^{30}\text{Si}_{\text{DSi}}$  composition of river waters reflect the processes occurring after silicate mineral dissolution (Opfergelt and Delmelle, 2012; Frings et al., 2016) resulting from secondary mineral formation and dissolution (Georg et al., 2006), adsorption of Si onto Al and Fe (oxy)hydroxides (Delstanche et al., 2009; Oelze et al., 2014), diatom uptake (Alleman et al., 2005; Opfergelt et al., 2011) and dissolution (Demarest et al., 2009; Egan et al., 2012; Wetzel et al., 2014) and phytolith formation (Opfergelt et al., 2008) and dissolution (Ziegler et al., 2005) in vascular plants during dissolved silicon transport in the river basin. At present,  $\delta^{30}\text{Si}_{\text{DSi}}$  compositions in large Arctic rivers are used to constrain the drivers of terrestrial-ocean silicon supply in high latitude permafrost-dominated systems with an average flux-weighted Arctic River  $\delta^{30}\text{Si}_{\text{DSi}}$  composition of +1.3‰ (Pokrovsky et al., 2013; Mavromatis et al., 2016; Sun et al., 2018). During winter months,  $\delta^{30}\text{Si}_{\text{DSi}}$  compositions are higher than average values, attributed to aluminosilicate dissolution and secondary mineral precipitation in groundwater systems (Pokrovsky et al., 2013). During spring flood, the  $\delta^{30}\text{Si}_{\text{DSi}}$  compositions are lower than or similar to silicate rock values, attributed to the dissolution of suspended matter within rivers and leaching of biomass (Pokrovsky et al., 2013; Mavromatis et al., 2016; Sun et al., 2018). During summer months,  $\delta^{30}\text{Si}_{\text{DSi}}$  compositions show a wide range in values resulting from Si uptake into vascular plants and phytoplankton alongside the mixing of tributaries with different Si isotope compositions (Sun et al., 2018). In these large river basins, the role of secondary mineral precipitation and its impact on riverine  $\delta^{30}\text{Si}_{\text{DSi}}$  compositions is often obscured by biological and plant uptake and/or mixing of surface and sub-surface waters in the river basin.

The simplified and well characterized MDV streams, with no vegetation and no groundwater supply to streams, provides an ideal natural laboratory to test whether the silicate mineral weathering release is affected by the formation secondary weathering products or by biological uptake of diatoms in a permafrost environment. To disentangle biogenic and non-biogenic contributions to rivers, the germanium/silicon ratio (Ge/Si) of river waters is complementary to Si isotopes (Cornelis et al., 2011). During weathering, Ge substitutes for Si during clay mineral formation resulting in soils with higher Ge/Si ratios and soil porewaters and rivers with lower Ge/Si ratios than the silicate parent material (Murnane and Stallard, 1990; Kurtz et al., 2002). During biological Si uptake by plants and diatoms, Ge is either unfractionated or fractionated with respect to Si to form biogenic amorphous silica with a Ge/Si ratio the same or lower than the starting solution (Froelich et al., 1992; Derry et al., 2005; Delvigne et al., 2009).

The  $\delta^{30}\text{Si}_{\text{DSi}}$  composition and the Ge/Si ratios are determined on waters in Crescent Stream, collected during three different seasons between 2014 and 2017, and at different times of day in

order to understand the effect of daily and seasonal variations in hydrology on silicate weathering in the hyporheic zone. Crescent Stream is one of the longest streams in Taylor Valley, resulting in longer water residence times in the hyporheic zone, increased chemical weathering and higher long-term solute concentrations compared to shorter streams in Taylor Valley (Wlostowski et al., 2018). Using these findings as a basis, we discuss how  $\delta^{30}\text{Si}_{\text{DSi}}$  compositions could be used to monitor changes in hyporheic zone functioning in response to future increases in stream flow (Doran et al., 2008), active layer depth (Doran et al., 2008), permafrost temperature (Biskaborn et al., 2019; Obu et al., 2020), and thermokarst erosion (Levy et al., 2013) in MDV.

## STUDY SITE

Samples were collected from Crescent Stream in Fryxell Basin, McMurdo Dry Valleys, Antarctica. The McMurdo Dry Valleys (77°S, 162°E) are located on the western coast of McMurdo Sound and have a polar desert environment with mean annual temperatures less than  $-15^{\circ}\text{C}$  and mean annual precipitation less than 100 mm (Doran et al., 2002). Soils are developed on glacial tills that were deposited by the grounded Ross Sea Ice Sheet in the Last Glacial Maximum, 19,000 to 23,000 years ago (Hall et al., 2000) and derived from granitic, sandstone and dioritic parent lithologies (Campbell and Claridge, 1987). There is 3–7% contribution of mafic material to Taylor Valley glacial tills derived from the McMurdo Volcanic Group and Ferrar Dolerite (e.g., Cooper et al., 2007). Soils are distinguished by the amount and distribution of salts and degree of chemical weathering. Permafrost is present across the McMurdo Dry Valleys with 43% characterized as dry frozen, 55% characterized as ice-cemented and 2% characterized as massive ice bodies (Bockheim, 2002). Active layer depths range from 45 to 70 cm in coastal areas to 20–45 cm in the polar plateau (Bockheim et al., 2007). There is no vascular vegetation in McMurdo Dry Valleys (Campbell and Claridge, 1987) and soil organic carbon concentrations are  $<0.5 \text{ mg C g soil}^{-1}$  (Burkins et al., 2001).

Dry-based glaciers are the main source of liquid water to McMurdo Dry Valleys. Supra-glacial meltwaters are transported via first-order streams to confined lake basins. Streams range from 1 to 11.2 km in length, are typically 5–10 m wide and incised in some places by up to 3 m (Conovitz et al., 1998). The extensive hyporheic zones of the streams are characterized by loose, unconsolidated sediments (Bockheim, 2002) and active layer depths up to 75 cm (Conovitz et al., 2006). The hyporheic zone extends several meters either side of the streambed, with a lateral cross section of  $\sim 12 \text{ m}^2$  at maximum thaw during the austral summer months (Gooseff et al., 2003). Microbial mats are abundant in MDV streams and are mainly found in streambed areas with flowing water and along stream margins that are submerged at occasional high flows (McKnight and Tate, 1997). The mats are dominated by filamentous cyanobacteria, with varying abundances of diatoms, chlorophytes and other microorganisms (Alger, 1997).

McMurdo Dry Valley stream flow occurs for approximately 6–10 weeks per year during the austral summer between

December and February and is characterized by inter-annual, seasonal and daily variations in discharge. Streams typically exhibit a low flow in December, maximum flow in January and low flow again at the start of February (McKnight et al., 1999). During cold and cloudy periods, there is intermittent stream flow and water is mainly accommodated in the hyporheic zone; whereas, warm and sunny periods drive more surface glacier melt and a larger volume of water is transported as stream flow (Conovitz et al., 1998). Daily diel flood pulses result in a 5–10 fold variation in stream flow depending on the solar aspect, insolation and air temperature (Conovitz et al., 1998).

Crescent Stream in the south Fryxell Basin, Taylor Valley (77°37'8.6"S, 163°11'4.1"E) transports meltwater from Crescent Glacier along two branches (east and west) that converge about 500 m upstream of where Crescent Stream discharges into Lake Fryxell (Figure 1).

## MATERIALS AND METHODS

### Sample Collection

Water samples were collected at gauging stage F8 (Figure 1), located 5.5 km downstream from Crescent Glacier (Gooseff and McKnight, 2019), during three austral seasons: 2014–2015 (2/1/2015 to 17/1/2015); 2015–2016 (11/12/2015 to 18/1/2016); and 2016–2017 (17/12/2016 to 24/1/2017) and at different times of day from 10.13 am to 11.58 pm. Water samples were collected in 1 L polyethylene bottles and filtered through 0.4  $\mu\text{m}$  Nucleopore filters using an Antlia filtration unit within 4–6 h after collection. Water samples were stored at  $>8^{\circ}\text{C}$ , but not frozen.

Discharge, conductivity and water temperature were measured at 15-min intervals at gauging stage F8 during the three austral seasons. Data are available on the LTER McMurdo Dry Valleys database, collecting data since 1990 (Gooseff and McKnight, 2019).

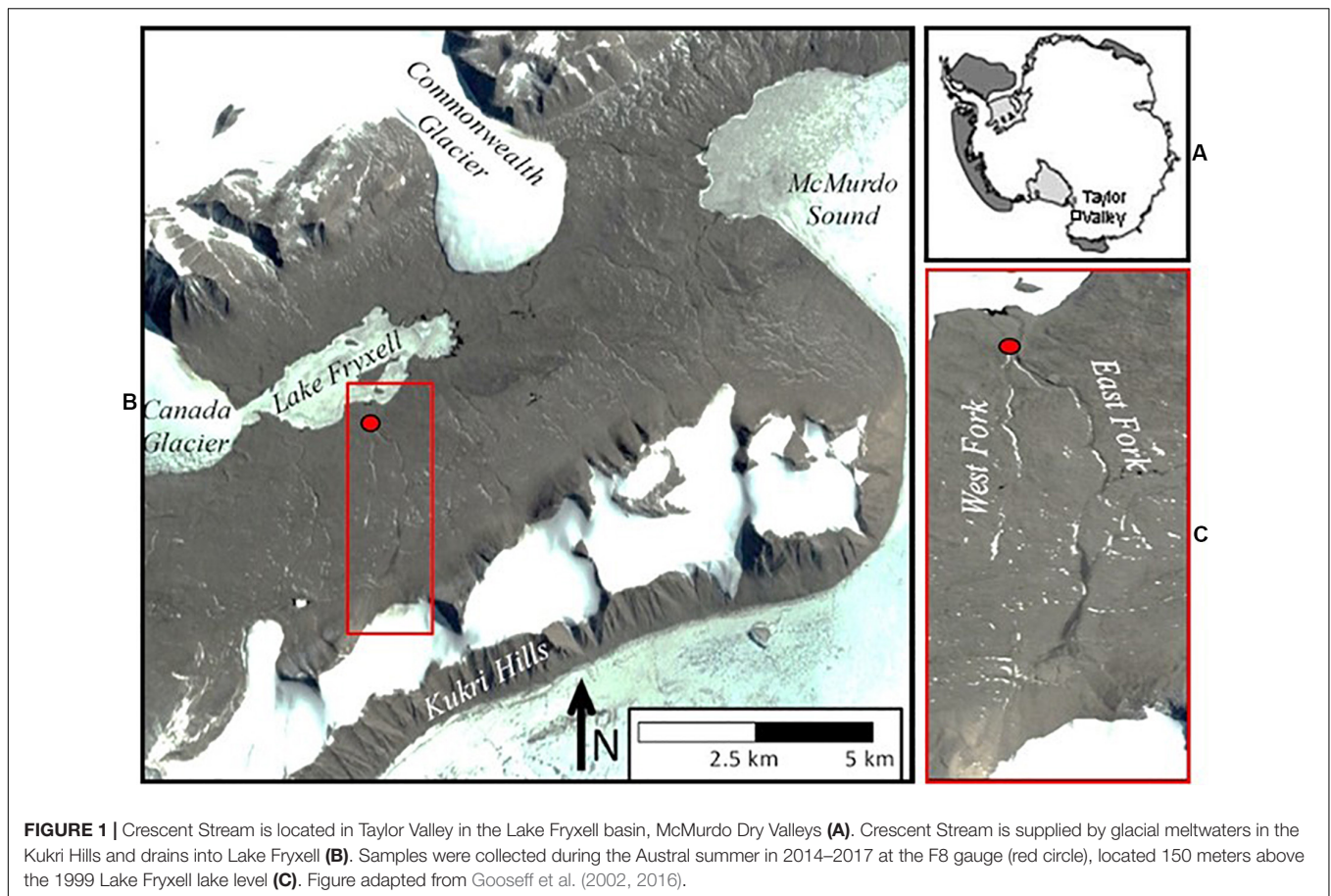
### Silicon Concentrations Analysis

Dissolved Si concentrations were determined on the water samples from Crescent Stream (austral summer seasons 2014–2015, 2015–2016, and 2016–2017) using a Skalar San++ nutrient analyzer at The Ohio State University, following the protocols of Mullin and Riley (1955). The precision of the Si concentrations and check standards, calculated as the average percent difference between duplicate samples, is  $<2\%$ . Blank values for DI water processed as a sample and stored in our clean bottles were always below the detection limit of the method.

### Germanium Concentrations Analysis

Ge concentrations were determined on the water samples from Crescent Stream (austral seasons 2014–2015, 2015–2016, and 2016–2017) by ICP-mass spectrometry (ICP-MS, ICAPQ Thermo Fisher Scientific) using the  $^{74}\text{Ge}$  isotope at Earth & Life Institute, UCLouvain, Belgium. Indium was used as the internal standard to correct for both instrumental (i.e., mass) drift, and sensitivity drift potentially arising from the sample matrix (Pretorius et al., 2006). The accuracy and





long-term reproducibility of the analysis were assessed by measuring two international riverine standards, namely SLRS-5 ( $[Ge] = 0.083 \pm 0.014 \text{ nmol.l}^{-1}$ ;  $n = 3$ ) and SLRS-6 ( $[Ge] = 0.097 \pm 0.0069 \text{ nmol.l}^{-1}$ ;  $n = 3$ ) (Yeghicheyan et al., 2001). The limit of detection for Ge was  $0.04 \text{ nmol.l}^{-1}$ , and the precision on Ge/Si ratio is 10%.

## Silicon Isotope Analysis

Silicon isotope compositions were determined on the water samples from Crescent Stream (austral seasons 2014–2015, 2015–2016, and 2016–2017). Si was pre-concentrated using MAGIC brucite precipitation (Brzezinski et al., 2003) with Si recoveries of 85 to 100%. Si was separated from the remaining anion-rich matrix with a two stage column chemistry procedure using an anion exchange resin (Biorad AG MP-1; Gaspard et al., 2019) followed by a cation exchange resin (Biorad AG50W-X12; Georg et al., 2006). Si recoveries were  $>95\%$  and  $\text{Na}^+$ ,  $\text{SO}_4^{2-}$  and  $\text{Cl}^-$  concentrations were below detection limit following the two-stage column chemistry. The combined procedural Si blank for MAGIC and column chemistry was below  $0.36 \mu\text{mol.l}^{-1}$ .

$\delta^{30}\text{Si}_{\text{DSi}}$  composition was analyzed by MC-ICP-MS (Neptune Plus<sup>TM</sup> High Resolution Multicollector ICP-MS, Thermo Fisher Scientific, Earth & Life Institute, UCLouvain, Belgium) in wet plasma mode in medium resolution ( $\Delta m/m \sim 6000$ ) using a PFA nebulizer of  $100 \mu\text{l/min}$  uptake rate. The instrumental

mass bias was corrected using the standard-sample bracketing technique and an external Mg doping (Cardinal et al., 2003). The analyses were performed in 2%  $\text{HNO}_3$  matrix, with a typical sensitivity of 7V for 2ppm Si and an instrumental blank  $<30 \text{ mV}$ .  $\delta^{30}\text{Si}_{\text{DSi}}$  compositions are expressed in relative deviations of  $^{30}\text{Si}/^{28}\text{Si}$  ratio from the NBS-28 reference standard using the common  $\delta$ -notation (‰) as follows:  $\delta^{30}\text{Si} = [(^{30}\text{Si}/^{28}\text{Si})_{\text{sample}} / (^{30}\text{Si}/^{28}\text{Si})_{\text{NBS-28}} - 1] \times 1000$ . One measurement comprises 30 cycles with 4.2s integration time corrected by blank in a 2%  $\text{HNO}_3$  matrix. Each single  $\delta$ -value ( $n$ ) represents one sample run and two bracketing standards.  $\delta^{30}\text{Si}$ -values are reported as the mean of isotopic analyses from multiple analytical sessions (Table 1). The  $\delta^{30}\text{Si}$  and  $\delta^{29}\text{Si}$  measurements fit within error onto the theoretical mass dependent fractionation array (Young et al., 2002) supporting the interference-free determination of all three Si isotopes via MC-ICP-MS (Supplementary Figure 1). The long-term precision and accuracy of the MC-ICP-MS  $\delta^{30}\text{Si}$  values was assessed from multiple measurements within each analytical session on reference materials: the values obtained for Diatomite ( $\delta^{30}\text{Si} = 1.31 \pm 0.08\text{‰}$ , SD,  $n = 21$ ) and Quartz Merck ( $\delta^{30}\text{Si} = -0.01 \pm 0.08\text{‰}$ , SD,  $n = 8$ ) are consistent with previously reported values for these standards [Quartz Merck:  $\delta^{30}\text{Si} = -0.01 \pm 0.12\text{‰}$  (Abraham et al., 2008); Diatomite:  $\delta^{30}\text{Si} = 1.26 \pm 0.10\text{‰}$  (Reynolds et al., 2007)].

**TABLE 1** | Sampling date, time, field measurements (discharge, conductivity, and water temperature), dissolved silicon and dissolved germanium concentrations, Ge/Si ratios, and silicon isotope compositions (SD) for all samples in this study collected in the austral seasons: 2014–2015, 2015–2016, and 2016–2017.

| Sample                      | Date       | Time | Discharge<br>L/sec | Conductivity<br>$\mu\text{S/cm}$ | Water temp<br>$^{\circ}\text{C}$ | Si<br>$\mu\text{mol L}^{-1}$ | Ge<br>$\text{pmol L}^{-1}$ | Ge/Si<br>$\mu\text{mol mol}^{-1}$ | $\delta^{29}\text{Si}$<br>‰ | SD<br>‰ | $\delta^{30}\text{Si}$<br>‰ | SD<br>‰ |
|-----------------------------|------------|------|--------------------|----------------------------------|----------------------------------|------------------------------|----------------------------|-----------------------------------|-----------------------------|---------|-----------------------------|---------|
| Crescent Stream F8 2/1/15   | 02-01-2015 | 1325 | 0                  | 253                              | 10.98                            | 136.1                        |                            |                                   | 0.65                        | 0.02    | 1.22                        | 0.07    |
| Crescent Stream F8 7/1/15   | 07-01-2015 | 1347 | 17                 | 185.4                            | 3.51                             | 99.2                         | 41.3                       | 0.41                              | 0.69                        | 0.03    | 1.24                        | 0.11    |
| Crescent Stream F8 13/1/15  | 13-01-2015 | 1855 | 0                  | 241.8                            | -0.73                            | 122.9                        | 41.3                       | 0.33                              | 0.68                        | 0.05    | 1.33                        | 0.08    |
| Crescent Stream F8 17/1/15  | 17-01-2015 | 1327 | 0                  | 152                              | 5.34                             | 117.3                        | 41.3                       | 0.34                              | 0.61                        | 0.06    | 1.23                        | 0.08    |
| Crescent Stream F8 11/12/15 | 11-12-2015 | 1209 | 0.38               | 133.6                            | 7.29                             | 142.7                        | 41.3                       | 0.28                              | 0.60                        | 0.05    | 1.13                        | 0.08    |
| Crescent Stream F8 14/12/15 | 14-12-2015 | 1425 | 50.97              | 206.2                            | 5.01                             | 89.3                         |                            |                                   |                             |         |                             |         |
| Crescent Stream F8 21/12/15 | 21-12-2015 | 1708 | 0.58               | 215.9                            | 9.77                             | 126.6                        | 41.3                       | 0.32                              | 0.60                        | 0.05    | 1.12                        | 0.07    |
| Crescent Stream F8 7/1/16   | 07-01-2016 | 1213 | 0.26               | 194.8                            | 7.79                             | 137.6                        |                            |                                   |                             |         |                             |         |
| Crescent Stream F8 12/1/16  | 12-01-2016 | 1319 | 0.93               | 208                              | 6.43                             | 136.4                        | 55.1                       | 0.39                              | 0.48                        | 0.03    | 0.90                        | 0.05    |
| Crescent Stream F8 16/1/16  | 16-01-2016 | 1753 | 9.07               | 139.4                            | 7.85                             | 112.7                        | 41.3                       | 0.36                              | 0.67                        | 0.08    | 1.25                        | 0.12    |
| Crescent Stream F8 18/1/16  | 18-01-2016 | 1753 | 43.71              | 174.1                            | 5.81                             | 111.2                        |                            |                                   |                             |         |                             |         |
| Crescent Stream F8 17/12/16 | 17-12-2016 | 1013 | 0.03               | 188.9                            | 1.3                              | 101.9                        | 55.1                       | 0.53                              | 0.57                        | 0.09    | 1.02                        | 0.10    |
| Crescent Stream F8 21/12/16 | 21-12-2016 | 1613 | 2.46               | 131.9                            | 4.27                             | 107.7                        | 41.3                       | 0.37                              | 0.73                        | 0.05    | 1.39                        | 0.09    |
| Crescent Stream F8 28/12/16 | 28-12-2016 | 1558 | 0.14               |                                  | 9.2                              | 130.2                        |                            |                                   | 0.68                        | 0.03    | 1.32                        | 0.07    |
| Crescent Stream F8 1/1/17   | 01-01-2017 | 2358 | 0.03               | 216.4                            | 2.64                             | 116.7                        | 55.1                       | 0.46                              | 0.52                        | 0.14    | 1.05                        | 0.13    |
| Crescent Stream F8 6/1/17   | 06-01-2017 | 1607 | 0.03               | 276.4                            | 11.51                            | 126.0                        |                            |                                   |                             |         |                             |         |
| Crescent Stream F8 11/1/17  | 11-01-2017 | 2358 | 3.96               | 101.2                            | 3.16                             | 116.7                        |                            |                                   |                             |         |                             |         |
| Crescent Stream F8 16/1/17  | 16-01-2017 | 2232 | 2.74               | 138.1                            | 4.63                             | 129.2                        |                            |                                   |                             |         |                             |         |
| Crescent Stream F8 24/1/17  | 24-01-2017 | 1600 | 1.86               | 39.6                             | 6.09                             | 115.5                        | 41.3                       | 0.35                              | 0.69                        | 0.06    | 1.31                        | 0.08    |

## Scanning Electron Microscopy

Sediment for SEM imaging was collected from Crescent Stream during the 2002–2003 austral summer, as described in Dowling et al. (2019). Briefly, samples were stored at room temperature after collection and were allowed to air dry. Samples were placed on carbon tape on an aluminum stub and then coated with gold/palladium with a Denton Desk V precious metal coater. Scanning electron microscopy was done with an FEI Quanta FEG 250 Field Emission SEM equipped with a Bruker EDX detector. Images were collected at 15 kV using either a secondary electron (SE) or back scattered electron detector (BSE).

## RESULTS

### Seasonal Variations in Field Parameters in Crescent Stream

For the austral seasons between 2014 and 2017, discharge, conductivity, and water temperature measurements ranged from 0 to 153 L/sec, 25–290  $\mu\text{S/cm}$ , and -2 to +12 $^{\circ}\text{C}$ , respectively (Table 1). These values lie within the range of long-term (1994–2014) measurements in Crescent Stream (Figure 2A, LTER McMurdo Dry Valleys database, Gooseff and McKnight, 2019). Discharge values were lowest during 2016–2017, when stream flow did not exceed 8.20 L/sec and highest during 2015–2016 when discharge reached 146 L/sec (Supplementary Figure 2A). The range of water temperature and conductivity values were similar for the three seasons (Supplementary Figures 2B,C). For the samples collected, discharge values ranged

from 0.0 to 57 L/sec (Table 1) and do not correspond with the pulses of peak seasonal discharge.

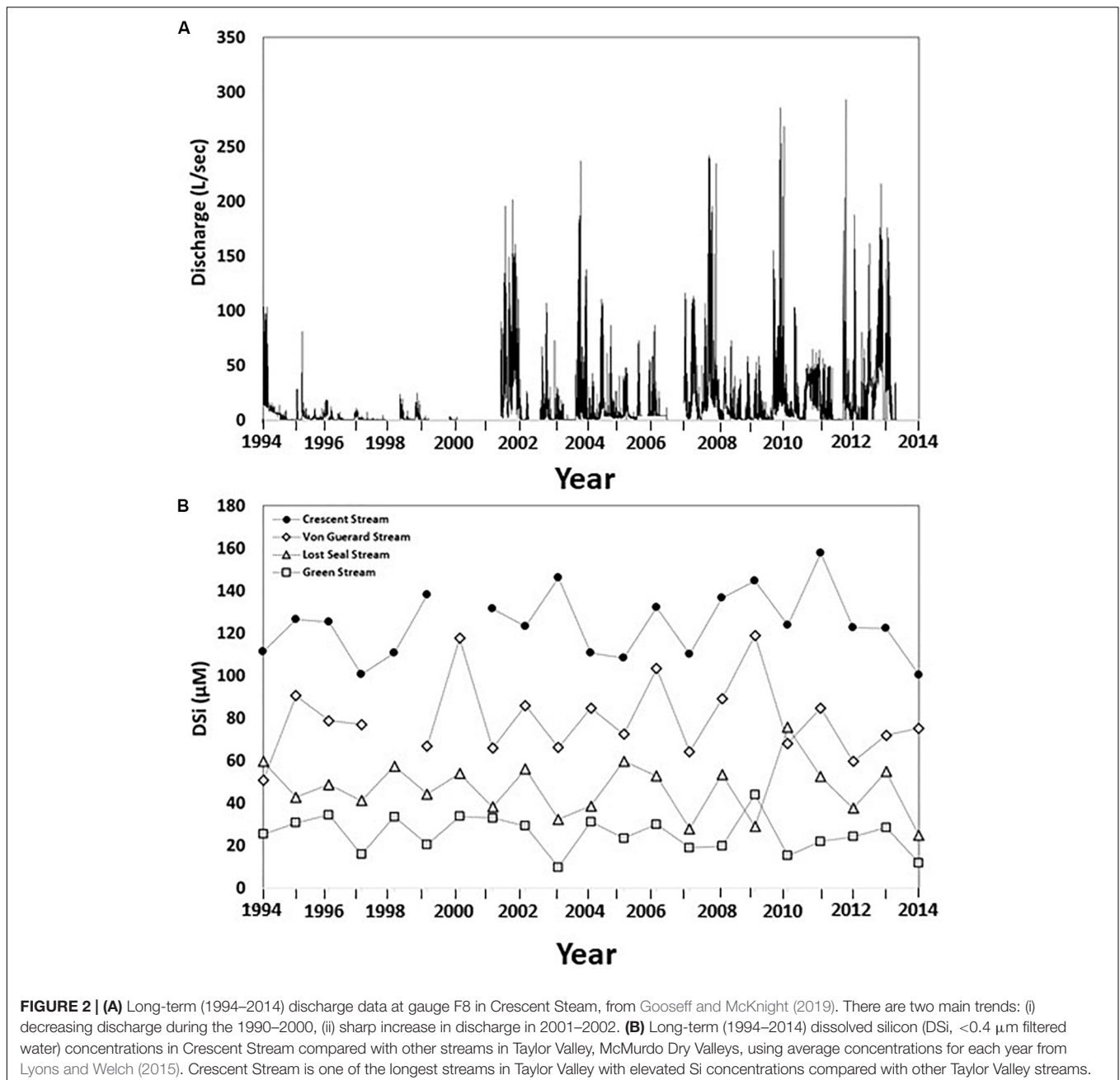
### Si Concentrations and Ge/Si Ratios in Crescent Stream

Si concentrations for samples collected in Crescent Stream ranged from 89 to 136  $\mu\text{M}$  between 2014 and 2017 (Figure 3 and Table 1). These values lie within the long-term (1994–2014) range of values measured in Crescent Stream, 83 to 163  $\mu\text{M}$  (LTER McMurdo Dry Valleys database, Lyons and Welch, 2015; Figure 2B). DSi concentrations show no relationship with long-term stream discharge data ( $R^2 = 0.01$ ) (Supplementary Figure 3) and no relationship with discharge data in the 2014–2017 austral summers ( $R^2 = 0.00$ ).

Germanium/silicon ratios (Ge/Si) in Crescent Stream ranged from 0.28 to 0.46  $\mu\text{mol mol}^{-1}$  for samples collected between 2014 and 2017 (Figure 4 and Table 1), lower than the range of Ge/Si values expected in silicate rocks (Bernstein, 1985). There was no significant variation in Si concentrations and Ge/Si ratios during the three austral summers, and no significant variation between these seasons.

### Silicon Isotope Compositions of Crescent Stream

Si isotope compositions ( $\delta^{30}\text{Si}$ ) in Crescent Stream ranged from +1.22‰ to +1.33‰ in 2014–2015, +0.90‰ to +1.25‰ in 2015–2016 and +1.02‰ to +1.39‰ in 2016–2017 (Figure 5 and Table 1), higher than  $\delta^{30}\text{Si}$  values in silicate rocks (Opfergelt and Delmelle, 2012). There was no significant variation in



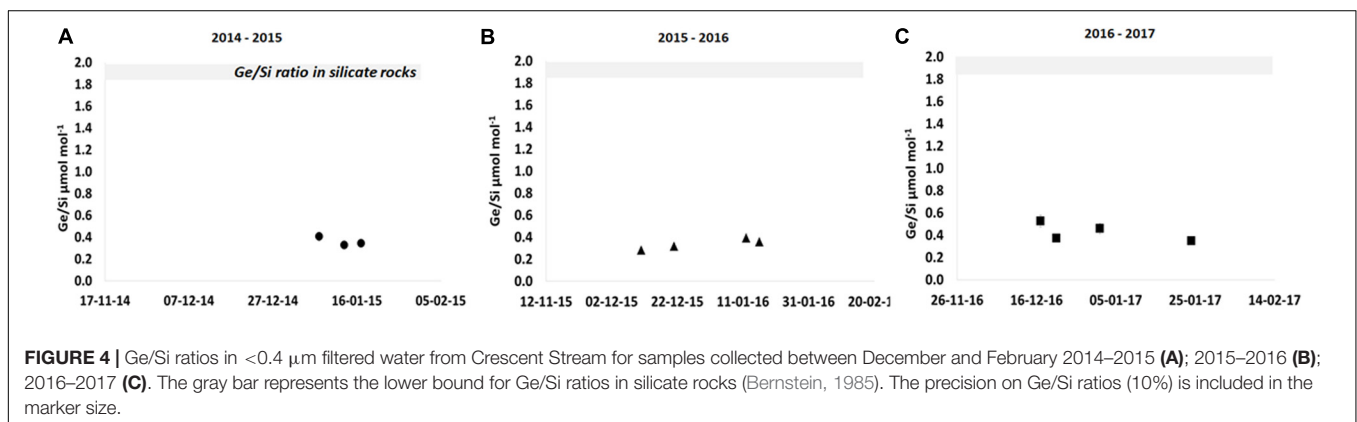
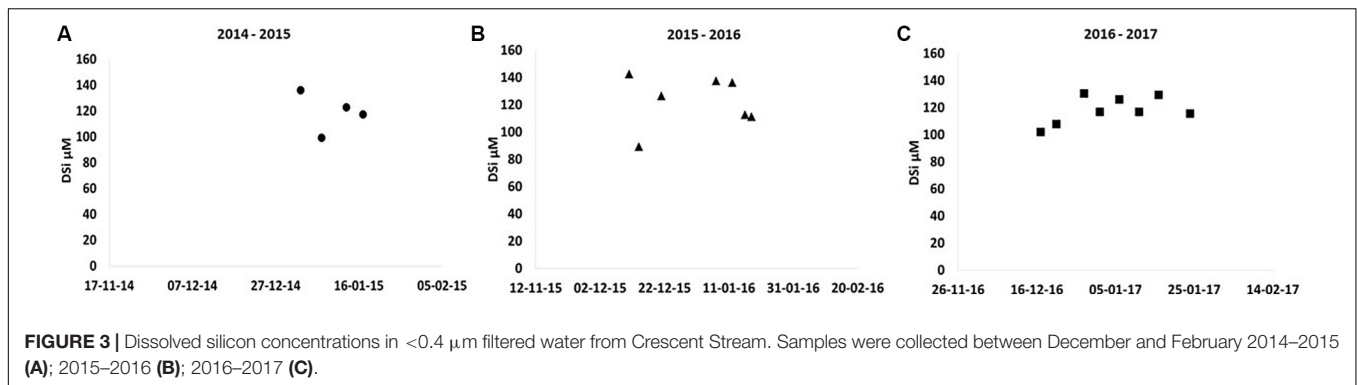
$\delta^{30}\text{Si}$  compositions during the three austral summers, and no significant variation between these seasons.

## Scanning Electron Microscope Images of Stream Sediment

Scanning Electron Microscope images of mineral grains from Crescent Stream sediments show that the sediment is composed of silicate-bearing minerals such as pyroxene, biotite, olivine and volcanic glass with preserved vesicles and non-silicate bearing minerals, including apatite grains and calcite grains (Figure 6). All minerals show evidence for chemical and physical alteration

of the mineral surface including linear etching over pyroxene and apatite mineral surfaces (Figures 6A,E), exfoliation of biotite minerals along a crystal plane (Figure 6B), etch pits and rounded facets on olivine mineral surfaces (Figure 6C), or extensive etching over calcite mineral surfaces (Figure 6D).

More specifically, volcanic ash spherules are associated with chemical alteration products in Crescent Stream sediments (Figure 7). SEM images show that spherules about 100 to 200 μm wide may present long cracks (~120 μm; Figure 7A) and a surface with a “sugary” texture, indicative of an alteration crust (Figure 7B). This crust is composed of micron-nano sized amorphous to poorly crystalline secondary minerals.



There is evidence of chemical alteration in fractured spherules, with coating patches on euhedral,  $\sim 5 - 10 \mu\text{m}$  long minerals (Figure 7C). A high-resolution SEM image of these patches indicates that these are hydrous or amorphous phases coating the surface of the euhedral minerals (Figure 7D).

## DISCUSSION

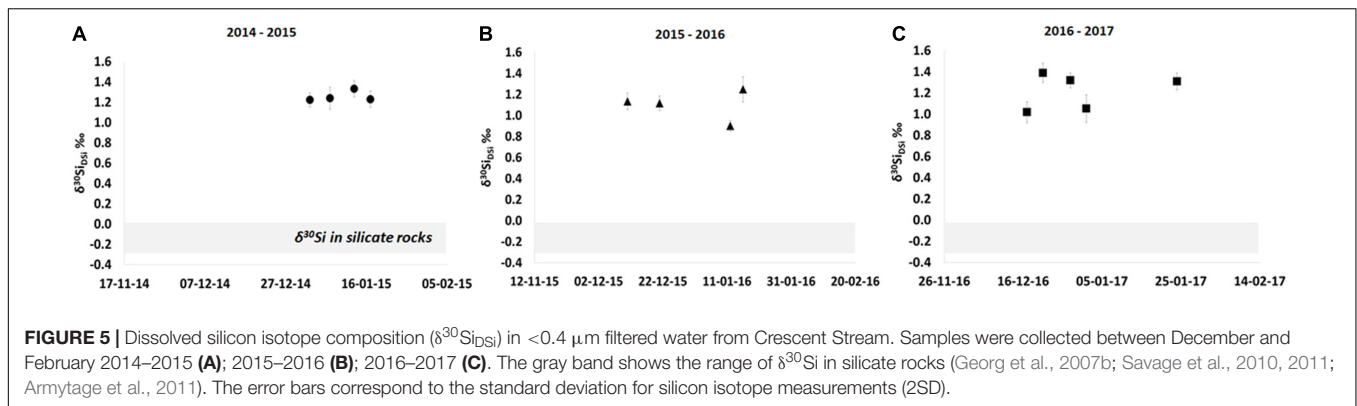
### Comparison Between Si Isotope Compositions in Crescent Stream, Permafrost-Dominated Rivers and Sub-Glacial Rivers

Glacial and permafrost-dominated river basins have contrasting weathering regimes (Anderson et al., 1997) resulting in contrasting dissolved silicon isotope compositions (Pokrovsky et al., 2013; Mavromatis et al., 2016; Sun et al., 2018; Hatton et al., 2019a,b). Figure 8A shows the Si concentrations and Si isotope composition of waters in sub-glacial meltwaters, permafrost-dominated Arctic Rivers and Crescent Stream (*this study*). Sub-glacial meltwaters have low DSi concentrations ranging from 3 to  $94 \mu\text{M}$  and  $\delta^{30}\text{Si}_{\text{DSi}}$  compositions ranging from  $-0.58\text{‰}$  to  $+0.87\text{‰}$ , attributed to amorphous Si and clay mineral dissolution during sub-glacial water-mineral interaction (Hatton et al., 2019a,b). Permafrost-dominated large Arctic Rivers have higher DSi concentrations ranging from 25 to  $310 \mu\text{M}$ , and  $\delta^{30}\text{Si}_{\text{DSi}}$  compositions ranging from  $+0.39\text{‰}$

to  $+2.72\text{‰}$  (Pokrovsky et al., 2013; Mavromatis et al., 2016; Sun et al., 2018). The wide scatter of compositions in large permafrost-dominated rivers prevents the isolation of a  $\delta^{30}\text{Si}_{\text{DSi}}$  signal from mineral weathering in permafrost soils.

Crescent Stream, MDV has a narrow range of DSi and  $\delta^{30}\text{Si}_{\text{DSi}}$  compositions, falling in a tight cluster within the range of values reported for Arctic Rivers (Figure 8A) showing that non-glacial weathering processes are contributing to  $\delta^{30}\text{Si}_{\text{DSi}}$  compositions in this Antarctic stream. In an attempt to connect permafrost-weathering conditions in Arctic and Antarctic streams, we compare  $\delta^{30}\text{Si}_{\text{DSi}}$  compositions in Crescent Stream with the  $\delta^{30}\text{Si}_{\text{DSi}}$  compositions for (i) wet-based glacial streams, (ii) Arctic rivers during winter baseflow, and (iii) Arctic rivers during the spring flood period (Figure 8B). Samples from the summer period (included in Figure 8A) are omitted because Si isotope fractionation during Si plant uptake obscures the weathering signal (Sun et al., 2018), a process that is not relevant in Antarctica. In the Arctic,  $\delta^{30}\text{Si}_{\text{DSi}}$  compositions during spring flood reflect DSi derived from dissolution of minerals and vegetation in the suspended load (Pokrovsky et al., 2013; Mavromatis et al., 2016; Sun et al., 2018) and so represent the bulk  $\delta^{30}\text{Si}$  composition of permafrost surface soils washed into the river during river ice-break up. In Figure 8B, the  $\delta^{30}\text{Si}_{\text{DSi}}$  compositions and DSi concentrations fall on a line that passes through this spring flood  $\delta^{30}\text{Si}_{\text{DSi}}$  composition, with the lowest  $\delta^{30}\text{Si}_{\text{DSi}}$  compositions in wet-based glacial streams attributed to secondary mineral dissolution (Hatton et al., 2019a) and highest  $\delta^{30}\text{Si}_{\text{DSi}}$  compositions during winter baseflow attributed





to secondary mineral formation in sub-permafrost groundwaters (Pokrovsky et al., 2013). The  $\delta^{30}\text{Si}_{\text{DSi}}$  compositions in Crescent Stream during the austral summer also fall on this line and are similar to  $\delta^{30}\text{Si}_{\text{DSi}}$  compositions for winter baseflow in Siberian rivers (Pokrovsky et al., 2013; Sun et al., 2018) suggesting that processes driving Si isotope fractionation during winter baseflow in Arctic Rivers likely also occur in Crescent Stream, Antarctica.

The Arctic River basins span a range of lithology, from basaltic (Kochehumo River, Pokrovsky et al., 2013) to terrigenous siliciclastic sediments (Lena River tributaries, Sun et al., 2018). However the distribution of DSi and  $\delta^{30}\text{Si}_{\text{DSi}}$  compositions during winter baseflow does not reflect lithology specific silicate-mineral weathering signatures but rather reflects the extent of secondary mineral formation and dissolution processes occurring in sub and supra-permafrost groundwaters in these Arctic basins (Pokrovsky et al., 2013).

The main pool of DSi entering Crescent Stream is derived from silicate mineral weathering in the hyporheic zone (Nezat et al., 2001; Gooseff et al., 2002; Maurice et al., 2002). The initial supra-glacial meltwaters have Si concentrations ranging from 4 to 8  $\mu\text{M}$  (Lyons et al., 1998; Nezat et al., 2001), contributing  $<10\%$  of the Si transported in Crescent Stream between 2014 and 2017. This glacially derived Si in MDV originates from stratospheric aerosols, aeolian salt and dust deposition onto glacier surfaces blown from the valley floor (Lyons et al., 2003). Assuming no isotope fractionation during mineral dissolution on the glacier surface, the DSi contribution to Crescent Stream from glacial waters will have  $\delta^{30}\text{Si}_{\text{DSi}}$  compositions within the array of basaltic to granitic  $\delta^{30}\text{Si}_{\text{DSi}}$  compositions (Savage et al., 2011). This allows us to use Si isotopes and Ge/Si ratios as a tracer of biotic and abiotic secondary mineral formation in the hyporheic zone and stream bed to constrain the processes that trap Si in the terrestrial system after being released from mineral dissolution.

## Si Cycling and Isotope Fractionation in the Hyporheic Zone of Crescent Stream

### Biotic Processes

Diatom growth preferentially incorporates the lighter Si isotopes, with an isotope fractionation factor,  $^{30}\epsilon$ , of  $-1.1\text{‰}$  for Si uptake in fresh water systems (Alleman et al., 2005; Opfergelt et al., 2011). Diatoms are substantial contributors to microbial mats

in most Taylor Valley streams (McKnight et al., 1998; Pugh et al., 2002; Esposito et al., 2008) with biogenic silica in modern and paleo diatoms making up 2–8% dry weight of stream sediments in meanders, pools and riffles (Heindel et al., personal communication). The microbial mats remain dormant during the winter months, are photosynthetically active within hours of the return of flow at the start of the austral summer (Howard-Williams et al., 1986) and mat biomass varies with seasonal flow patterns with loss due to scouring of the mats occurring during high flow (Stanish et al., 2011; Cullis et al., 2014) over the austral summer. In streams with lower annual discharge, which are generally longer and have higher DSi concentrations, the larger more silicified diatom taxa, such as *Hantzchia* spp. (about 100  $\mu\text{m}$  in length), are more abundant; whereas *Psammothidium* spp. and other smaller taxa (about 12  $\mu\text{m}$  in length) are common in streams which have higher annual flows and are usually shorter with lower DSi concentrations (Stanish et al., 2011). In general, because smaller cells have a higher surface area to volume ratio and would be better able to meet their Si requirement for growth, this suggests that DSi availability may influence the diatom community composition, but the DSi does not limit diatom growth rate. Diatom growth can therefore contribute to the uptake of a fraction of mineral-derived DSi over the austral summer months.

The diatom community composition at the study site in the lower reaches of Crescent Stream was similar in the summer of 2014 and 2016 for both the black mats that grow at the stream margin and the orange mats that grow in the main channel (**Supplementary Table 1**). The species richness of these samples ranged from 9 to 20, which is typical for microbial mats in Dry Valley streams. A distinctive aspect of the diatom community in these mats was the consistent dominance by the monoraphid diatom *Achnanthes taylorensis*, which accounted for 41% or more of the total diatom cells counted. This species ranges in length from 25 to 38  $\mu\text{m}$  and is commonly present at relatively low abundance (a few percent or less) in microbial mats in streams adjacent to Crescent Streams (Spaulding et al., 2020). However, this species has been found to be more abundant in microbial mats in the nearby Spaulding Pond at the base of the Howard Glacier and in a few ponds at Cape Royds across McMurdo Sound. Furthermore, *A. taylorensis* was common in the hyporheic sediments studied in the adjacent Von Guerard



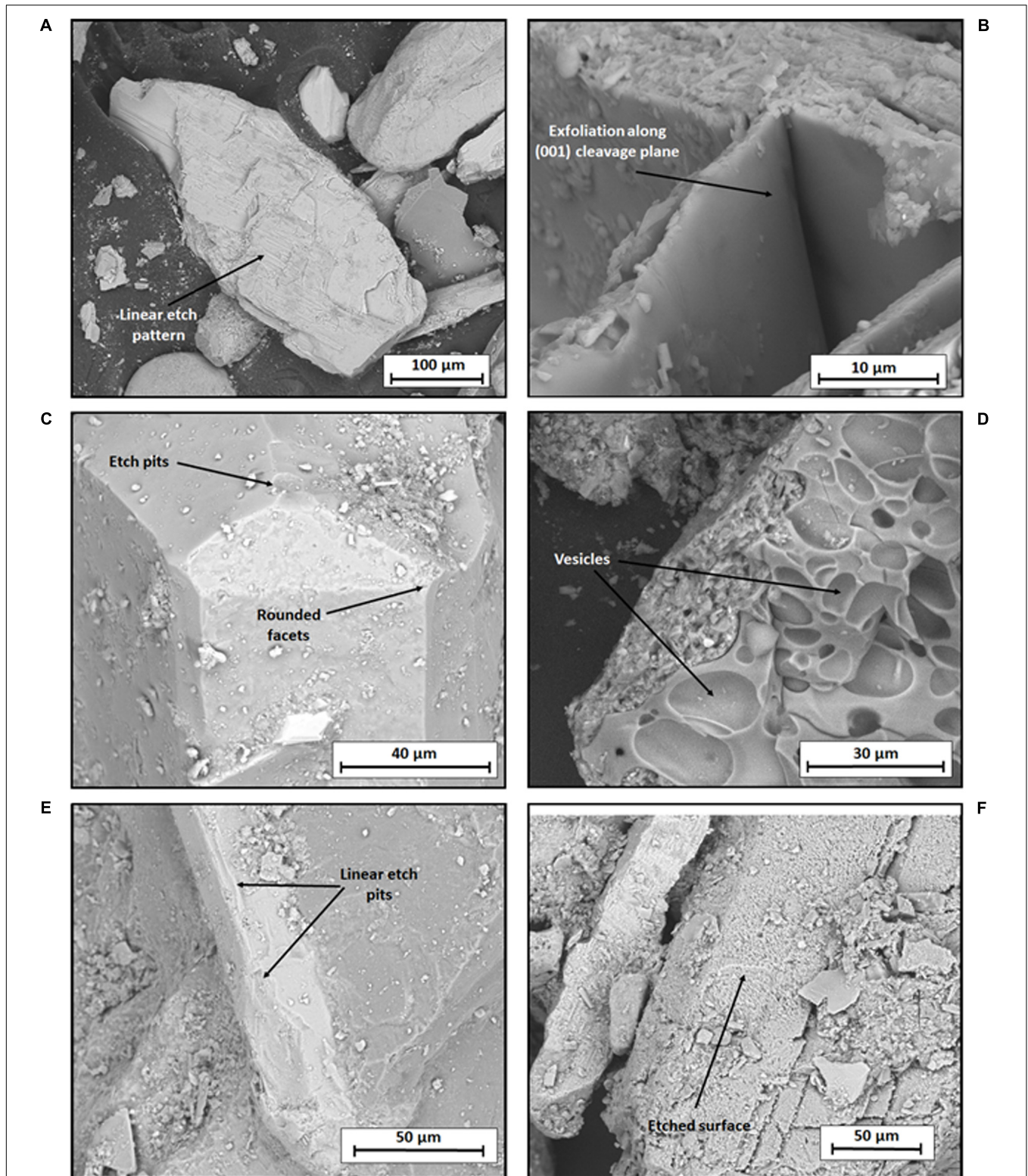
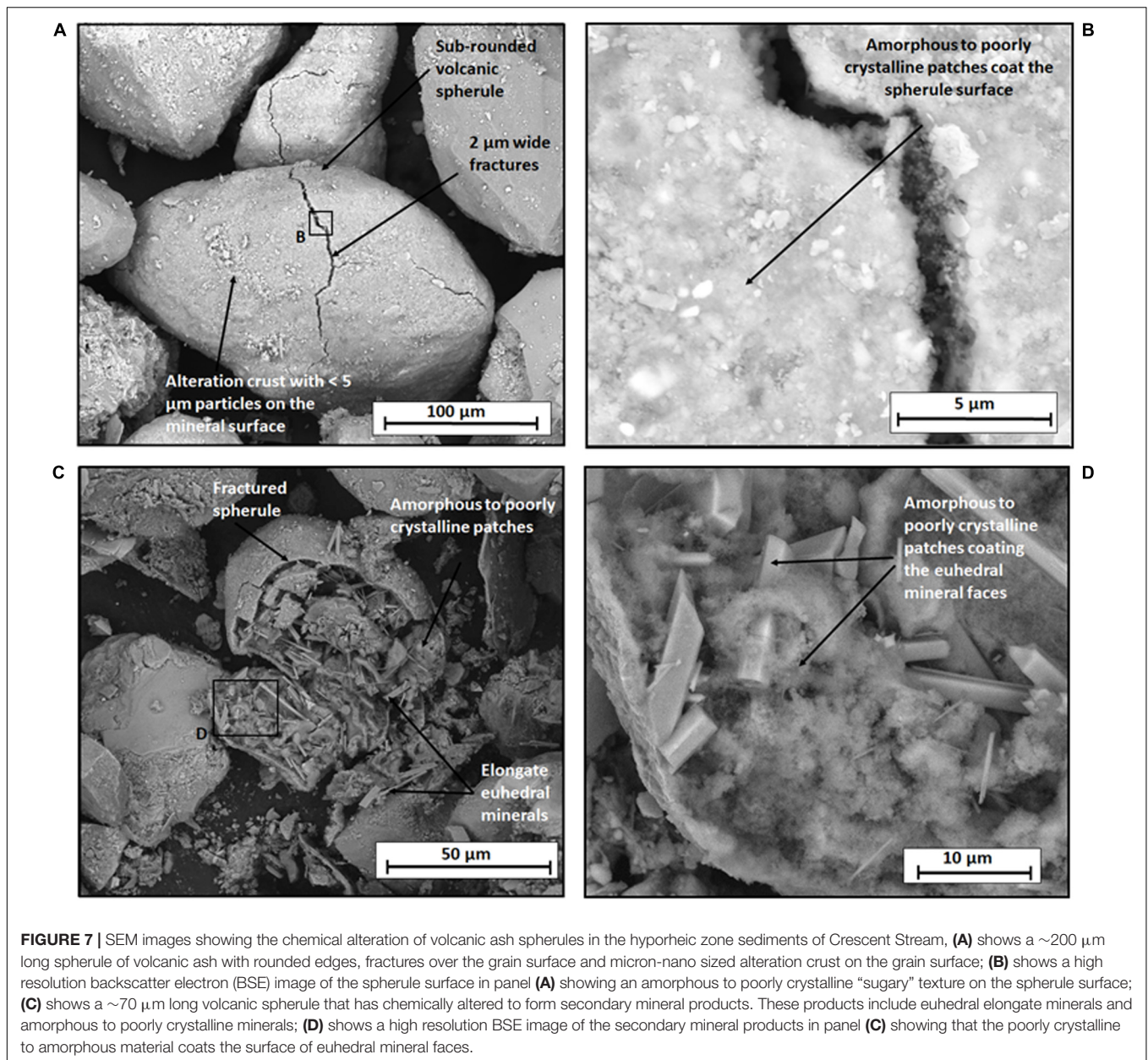


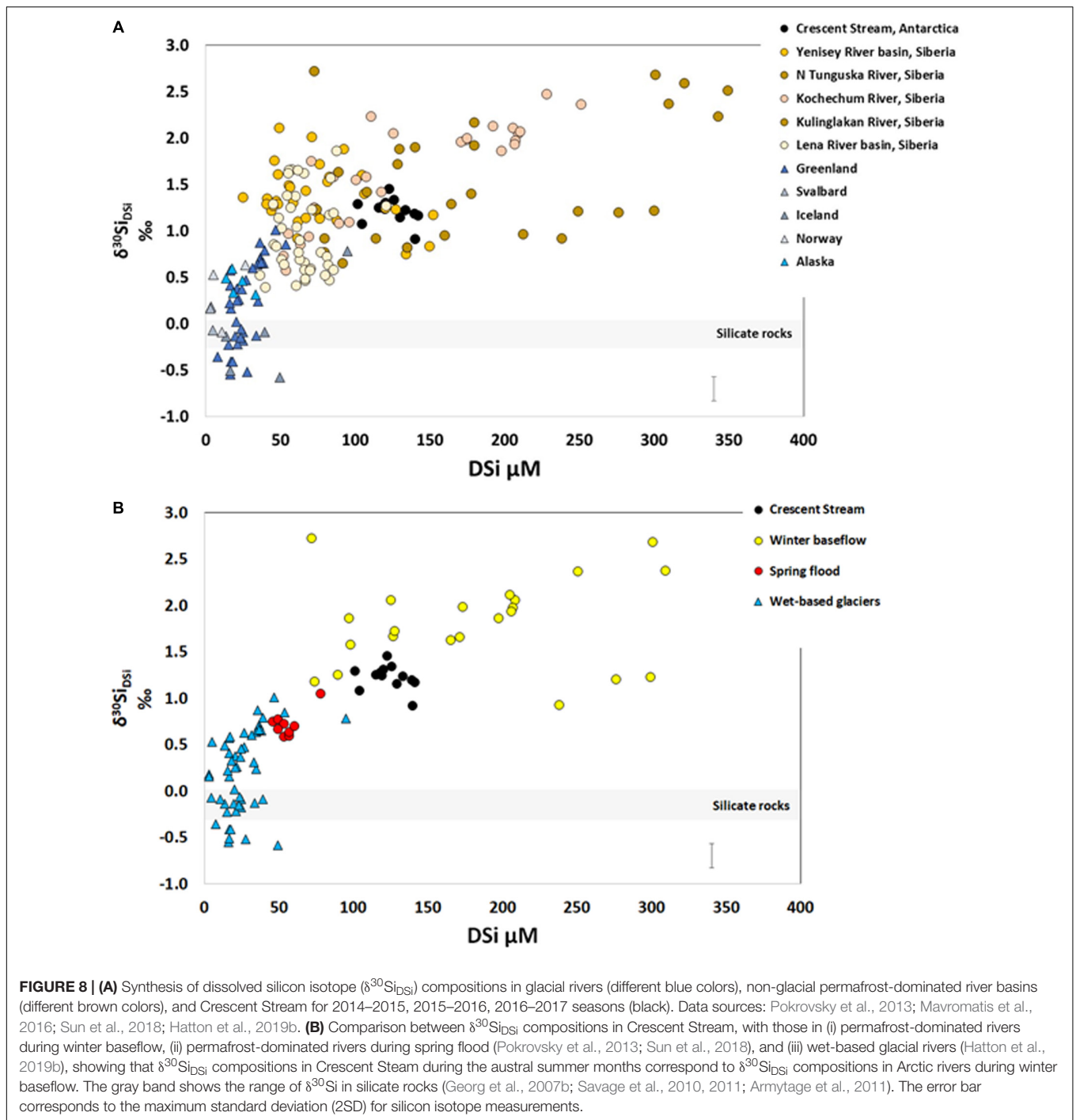
**FIGURE 6** | SEM images of minerals in the hyporheic zone sediments of Crescent Stream, including silicate-bearing minerals (A–D) and calcium and phosphate bearing minerals (E,F). (A) shows a large (300  $\mu\text{m}$  long) euhedral pyroxene grain with physical abrasions and linear etched pattern on the surface; (B) shows a biotite grain with physical alteration and exfoliation along the (001) cleavage plane; (C) shows an olivine grain with a euhedral surface, slightly rounded facets and few small etch pits on the surfaces; (D) shows volcanic glass and ash with a vesicular surface and coating of fine grained amorphous-nanocrystalline on the left side of the glassy particle surface; (E) shows an elongate apatite grain with crystallographically controlled etch pits; (F) shows calcite minerals with extensively etched surfaces.



Stream (Heindel, unpublished data). Another distinctive aspect of the diatom community is the relatively low abundance of *Hantzschia* species, which are large highly silicified taxa commonly abundant in mats in adjacent streams. There were a total of 11 species of the genus *Luticola* found in these mat samples, which is typical for these streams. It is interesting that *L. dolia* and *L. elegans* were relatively more abundant among the *Luticola* species than is typical for the diatom communities in adjacent streams. Overall, these results confirm that benthic diatoms were present in microbial mats in Crescent Stream during the sampling period and that the dominant diatom taxa is known to accumulate in hyporheic sediments in another adjacent stream. Here we discuss the extent to which DSi incorporation into diatoms contributes to the sequestration of

primary mineral derived-DSi and the high  $\delta^{30}\text{Si}_{\text{DSi}}$  compositions in Crescent Stream.

The extent to which Si isotope fractionation during DSi uptake is sufficient to impact the  $\delta^{30}\text{Si}_{\text{DSi}}$  in the stream water depends on the Si demand from the diatom growth relative to the rate of silicate mineral dissolution in the hyporheic zone. If the rate of production from silicate mineral dissolution is greater than the rate of uptake by diatoms, the Si concentration would still increase in the downstream direction but at a lower rate. Thus, the DSi concentration would not necessarily decrease downstream if diatom uptake were influencing the  $\delta^{30}\text{Si}_{\text{DSi}}$  composition. A synoptic study of downstream patterns of Si concentrations in Von Guerard Stream shows that Si weathering rates were similar for moderate and low flow streams



(Gooseff et al., 2002) suggesting that an additional process, such as increased microbial mat growth during low to moderate stream flow (Stanish et al., 2011) sequesters a portion of the DSi in streams. This is evidence to show that diatoms incorporate a relatively significant portion of the DSi released from silicate weathering in hyporheic zone sediments in MDV stream. Diatom growth rates in the laboratory are slow and independent of temperature for four of the dominant diatoms isolated from the MDV, which could support a stable biotic Si uptake rate per area

of microbial mat in the streams (Darling et al., 2017) over the duration of the austral summer, consistent with the relatively constant  $\delta^{30}\text{Si}_{\text{DSi}}$  compositions (Figure 5).

Here we use Ge/Si ratios to understand the extent to which the DSi, released via silicate weathering, is taken up into diatoms in Crescent Stream. Diatoms generally do not discriminate between Ge and Si during growth i.e., the Ge/Si ratio of diatom opal reflects that of ambient water (Froelich et al., 1992). The exception to this occurs at low DSi concentrations where diatoms



might start to discriminate against Ge, therefore raising the Ge/Si ratio in water (Sutton et al., 2010). The use of Ge/Si ratios to understand Si uptake into diatoms is difficult in Arctic river basins draining organic-rich permafrost soils because a portion of the Ge released from silicate weathering can form complexes with dissolved organic carbon (DOC) (Pokrovski and Schott, 1998). The contribution of Ge-organic complexes can be considered as limited in Crescent Stream given that the DOC concentrations in the MDV is low ( $<50 \mu\text{M}$ ; Gooseff et al., 2002), except for an initial pulse when the streams are first wetted. Therefore, we can be confident to use the Ge/Si ratio in this Antarctic stream without being concerned about Ge-Si fractionation by organic colloids, such as in boreal rivers (Pokrovski and Schott, 1998). If only diatom uptake is mediating the net DSi concentrations and  $\delta^{30}\text{Si}_{\text{DSi}}$  compositions, Ge/Si should stay the same (Froelich et al., 1992) or increase relative to the silicate rock ratio at low DSi concentrations (Sutton et al., 2010). However, Ge/Si ratios are lower than in silicate rocks (Figure 4; Bernstein, 1985) showing that DSi uptake into diatoms could contribute to increase  $\delta^{30}\text{Si}$  compositions relative to the signature of silicate rocks but is not the only mechanism behind the heavy  $\delta^{30}\text{Si}_{\text{DSi}}$  compositions in Crescent Stream.

An additional supply of DSi from diatom dissolution in hyporheic zone sediments must also be accounted for when considering the net contribution of diatoms to the silicate weathering flux. Diatom dissolution preferentially releases the lighter Si isotope, with an isotope fractionation factor,  $^{30}\epsilon$ , of  $-0.55\text{‰}$  (Demarest et al., 2009) in fresh water systems. Thus the dissolution of diatoms in the hyporheic zone would act to lower  $\delta^{30}\text{Si}_{\text{DSi}}$  compositions in streams. During the austral summer months, there is a continuous input of diatoms in the particulate organic matter entering the hyporheic zone from upstream scouring events (Cullis et al., 2014). From a mass balance perspective, the present-day quantity of modern diatoms in hyporheic zone sediments can be explained by (i) the continuous supply of diatoms to sediments from microbial mats upstream and (ii) dissolution of diatoms in the hyporheic zone sediments. However, the high  $\delta^{30}\text{Si}_{\text{DSi}}$  compositions in Crescent Stream indicate that diatom dissolution likely had a negligible contribution to silicate weathering rates in Crescent Stream between 2014 and 2017.

The combined evidence shows that only a fraction of DSi released from silicate mineral weathering is taken up by diatoms growing on the stream bed, resulting in a constant background supply of DSi (in equilibrium with diatoms) with higher  $\delta^{30}\text{Si}_{\text{DSi}}$  compositions to Crescent Stream during austral summer months.

## Abiotic Processes

### *Silicon incorporation in secondary weathering products*

Clay minerals preferentially incorporate the lighter Si isotopes, with isotope fractionation factors varying from  $-1.8\text{‰}$  to  $-2.0\text{‰}$  (Opfergelt and Delmelle, 2012) driving  $\delta^{30}\text{Si}_{\text{DSi}}$  compositions in soil porewaters to heavier values (Georg et al., 2007a). In MDV, hyporheic waters are oversaturated with respect to kaolinite (Gooseff et al., 2002) and some secondary products (kaolinite, illite and smectite) have been observed in the fine fraction ( $<2 \mu\text{m}$ ) of hyporheic zone sediments (Lyons et al.,

1998; Gooseff et al., 2002), with some controversy raised about their extent (Lyons et al., 1998). SEM images of sediments in Crescent Stream show micron-sized clay minerals on the surface and within broken volcanic spherules (Figures 7A,C), suggesting that a fraction of DSi released during primary mineral weathering is incorporated into clay minerals on altered mineral surfaces. Volcanic spherules contribute  $<1\%$  of Crescent Stream sediments (Dowling et al., 2019) but are subject to extensive chemical and physical alteration (Figure 7) and are likely an important site for secondary clay mineral formation in Crescent Stream sediments.

Here we use Ge/Si ratios to confirm that clay mineral formation is occurring during meltwater-sediment exchange in Crescent Stream between 2014 and 2017. Ge/Si ratios in Crescent Stream range from 0.28 to  $0.53 \mu\text{mol mol}^{-1}$  (Figure 4) which is lower than Ge/Si ratios in silicate rocks ( $1-3 \mu\text{mol mol}^{-1}$ , Bernstein, 1985) suggesting that a fraction of DSi released from parent materials is incorporated into clay minerals during water transport in Crescent Stream. Ge/Si ratios would also decrease if amorphous silica (ASi) dissolution occurs providing Si and not Ge to stream waters. However, it is unlikely that significant ASi dissolution occurs because this would also decrease the  $\delta^{30}\text{Si}$  of DSi (Li et al., 1995).

The Ge/Si ratios in the samples collected between 2014 and 2017 were relatively similar, with no obvious trends throughout the season or over the 3 years of samples collected. There are no seasonal or daily variation in Ge/Si ratios (Figure 4), consistent with the evidence showing that meltwaters are in chemical equilibrium with mineral surfaces during transport in the hyporheic zone (Wlostowski et al., 2018). Under these weathering conditions, any changes in Ge and Si supply from the water-clay mineral interface during the austral summer are dependent on water transit times rather than variations in clay mineral formation showing that DSi is in equilibrium with clay minerals and supplies a constant background  $\delta^{30}\text{Si}_{\text{DSi}}$  composition to Crescent Stream during the 2014–2017 austral summers.

Additional Si isotope fractionation may occur via preferential absorption of lighter Si isotopes onto Fe and Al (oxy)hydroxides (Delstanche et al., 2009; Opfergelt et al., 2009; Oelze et al., 2014). Moreover, Ge may be sequestered on Fe (oxy)hydroxides (Scribner et al., 2006) and also contribute to the low Ge/Si ratios in Crescent Stream. The quantity of Fe (oxy)hydroxides and Al oxides in stream sediments and conditions for element absorption during glacial meltwater-sediment exchange are poorly understood. However, the fine sediment fraction ( $<2 \mu\text{m}$ ) is made up of 40–65% by weight of amorphous weathering products (Gooseff et al., 2002). This amorphous fraction only represents 0.3 wt% of the bulk sediment (Gooseff et al., 2002) but is distributed over the primary mineral surfaces in Crescent Stream sediments (Dowling et al., 2019). That fraction may contain amorphous to poorly crystalline Fe oxy-hydroxides that contribute to the high  $\delta^{30}\text{Si}_{\text{DSi}}$  compositions in Crescent Stream.

### *Cryogenic amorphous silica precipitation*

In Crescent Stream, MDV, the high  $\delta^{30}\text{Si}_{\text{DSi}}$  compositions cannot be controlled by silicate mineral dissolution only and clay mineral formation likely contributes to modify the silicate rock



signal. Amorphous silica precipitation is an additional important process that has to be considered in this environment, which is subjected to sub-zero temperatures for the majority of the year with mean annual temperatures between  $-17^{\circ}\text{C}$  and  $-20^{\circ}\text{C}$  (Doran et al., 2002).

At the freezing point of waters in soils and sediments, ice formation occurs and DSi is concentrated in the surrounding brines (Channing and Butler, 2007). If Si saturation occurs, up to 90 mol% of the starting DSi can be precipitated as amorphous silica (Dietzel, 2005) and Si is fractionated with an isotope fractionation factor,  $^{30}\epsilon$ , of  $-1.0\text{‰}$  (Li et al., 1995). This occurs either by a steady-state fractionation where the final solid has the same Si isotope composition as the starting fluid (assuming all DSi precipitates),  $\Delta^{30}\text{Si}_{\text{solid-hyporheic zone solution}} = [\delta^{30}\text{Si}_{\text{solid}} - \delta^{30}\text{Si}_{\text{hyporheic zone solution}}] \approx 0\text{‰}$ ; or by unidirectional kinetic isotope fractionation where the final solid has a lighter isotope composition than the starting fluid,  $\Delta^{30}\text{Si}_{\text{solid-hyporheic zone solution}} \approx <0\text{‰}$  (Frings et al., 2016 and references therein). This is assuming no re-equilibration of Si isotopes in amorphous silica after precipitation (Fernandez et al., 2019). Unidirectional kinetic isotope fractionation occurs if (i) there is a closed system with no Si inputs or outputs; (ii) there is no change to the  $\delta^{30}\text{Si}$  composition of DSi in the starting solution; (iii) dissolved Al concentrations are greater than 0.1 mM (Li et al., 1995; Oelze et al., 2015; Frings et al., 2016). Under these conditions, amorphous silica precipitation during cryogenic precipitate formation in permafrost soils can fractionate Si isotopes and drive riverine  $\delta^{30}\text{Si}_{\text{DSi}}$  compositions to heavier values. This process has been invoked to explain the heavier Si isotope compositions in large Arctic rivers during winter months (Pokrovsky et al., 2013) and heavy Si isotope in soils porewaters in seasonally frozen Icelandic soils (Opfergelt et al., 2017).

In Crescent Stream, glacial meltwaters are transported along preferential flow paths in isolated areas of the hyporheic zone (Cozzetto et al., 2013) and water can collect in these isolated pockets at periods of high flow during the austral summer and when flow stops at the end of the austral summer (Cozzetto et al., 2006). The waters in the hyporheic zone and active layer soils freeze, likely at temperatures below  $0^{\circ}\text{C}$  because of the high concentrations of salts. During freezing and ice formation, dissolved Si accumulates in surrounding unfrozen waters and dissolved Si becomes saturated with respect to amorphous silica. Si isotope fractionation occurs by unidirectional kinetic isotope fractionation preferentially incorporating the light isotopes in amorphous silica and leaving a heavy Si isotope composition in surrounding waters. SEM images of sediments in Crescent Stream (Figures 7B,C) suggest the presence of an amorphous mineral phase on the surface of primary minerals. This phase may be composed of amorphous silica suggesting that amorphous silica precipitation occurs in hyporheic zone sediments in Crescent Stream. Assuming there are no freeze-thaw cycles, the heavy isotope signal remains trapped in the isolated pockets during the winter months and this preserved signal may contribute to the high  $\delta^{30}\text{Si}_{\text{DSi}}$  compositions of Crescent Stream in the austral summer months.

The contribution of a winter-derived  $\delta^{30}\text{Si}_{\text{DSi}}$  signal to stream water  $\delta^{30}\text{Si}_{\text{DSi}}$  over the austral summer months depends on the

rate at which these winter waters exchange with Crescent Stream waters. Evidence from  $\delta^{18}\text{O}$  and  $\delta\text{D}$  compositions suggests that winter waters are flushed from the hyporheic zone at the start of the austral summer and not continuously supplied over the summer months (Gooseff et al., 2003). In early December, water in the extended hyporheic zone have enriched  $\delta^{18}\text{O}$  and  $\delta\text{D}$  compositions resulting from evaporation and sublimation in the previous winter and summer. At the start of the austral summer, this enriched signal is transferred to stream waters providing evidence for early season hyporheic-stream water exchange. Gooseff et al. (2003) show that stream water  $\delta^{18}\text{O}$  and  $\delta\text{D}$  enrichment decreased substantially between the first sampling date (Dec 7) at the beginning of flow, and the subsequent dates during the main flow period (Dec 21 and Jan 7), indicating that the relative contribution of waters from the extended hyporheic decreases in the 1st weeks of the austral summer.

Further, we can place physical constraints on how much water with a heavy  $\delta^{30}\text{Si}_{\text{DSi}}$  can enter the stream from the hyporheic zone. The volumetric content of unfrozen water in the hyporheic zone was 10% at the end of the summer (Wlostowski et al., 2018). We can calculate a high estimate for the potential volume of the hyporheic zone for Crescent Stream as  $5\text{ km} \times 0.2\text{ m} \times 10\text{ m}$  (stream length  $\times$  hyporheic zone depth  $\times$  width) to be  $10 \times 10^6$  L. Using these estimates of unfrozen water content and hyporheic zone volume we estimate that  $10^6$  L of water is present in the hyporheic zone at the end of the Austral summer months. Given the rapid hyporheic exchange, we can estimate how fast that volume would be flushed out of the near and extended hyporheic zone contributing 10% of the water at a low flow rate in the stream of 10 L/sec (Supplementary Figure 2), corresponding to 1 L/sec. As a result, it can be estimated  $10^6$  L of water would take  $10^6$  sec or about 12 days to be flushed out at a flow rate of 1 L/sec. The 10 L/sec flow rate is a low value and flushing could happen more rapidly with higher flows. These constraints are consistent with evidence from  $\delta^{18}\text{O}$  and  $\delta\text{D}$  compositions (Gooseff et al., 2003) and show that winter waters are flushed out of the extended hyporheic zone at the beginning of the austral summer.

Consistent with this evidence for an early season flushing of winter waters, we could therefore expect to observe an increase in DSi and  $\delta^{30}\text{Si}_{\text{DSi}}$  compositions at the start of summer. However, this early season pulse is not observed in the samples collected at the start of the austral season (December 11th to December 28th, Table 1). One scenario is that early season sampling did not coincide with the release of waters stored in the hyporheic zone over the austral winter. For all seasons, sampling began 0–6 days after the onset of river discharge (Supplementary Figure 2A, LTER McMurdo Dry Valleys database, Gooseff and McKnight, 2019). Considering that active layer thaw coincides with glacial surface melt at the start of the austral summer (Gooseff et al., 2002), the collected samples likely coincided with the onset of hyporheic zone development and thus would capture the early release of waters stored during winter months. To improve on this effort, a high resolution (e.g., daily) sampling during early season thaw is required to detect a winter-derived  $\delta^{30}\text{Si}_{\text{DSi}}$  signal. A second scenario is that the winter-derived DSi made up a relatively small fraction of the total DSi in Crescent Stream, and the pulse of DSi with high  $\delta^{30}\text{Si}_{\text{DSi}}$

compositions did not affect the relatively constant stream Si isotope composition. Alternatively, to explain a constant supply of winter-derived high  $\delta^{30}\text{Si}_{\text{DSi}}$  compositions to Crescent Stream, we consider the entire hyporheic zone as individual “nested storage zones with unique timescales of exchange” (Gooseff et al., 2003). In this scenario, the nested storage zones each represent pockets of frozen sediment at the start of the austral summer. During gradual thaw over several weeks between December and January (Conovitz, 2000), the pockets of unfrozen water associated with amorphous silica are incrementally unlocked and the unfrozen water is connected to the stream during sediment-stream water exchange. In this hypothesis, the high  $\delta^{30}\text{Si}$  compositions are gradually added to the stream waters as the hyporheic zone is established over the summer months. Further work is required to understand the development of winter-derived  $\delta^{30}\text{Si}_{\text{DSi}}$  compositions and their contribution to summer river waters in permafrost dominated-basins.

A conceptual model of these processes is presented in **Figure 9**, highlighting the processes driving Si isotope fractionation in the hyporheic zone, which are visualized as individual segments of water–mineral interactions. The  $\delta^{30}\text{Si}_{\text{DSi}}$  compositions in waters collected at Gauge F8 in Crescent Stream results from the mixing of DSi from pockets of the hyporheic zone, influenced by amorphous silica formation during winter months, by diatom growth during summer months and ongoing clay mineral formation in these sediments. In this system,

DSi concentrations increase as hyporheic zone pockets are connected with stream water but there is no evolution of the silicon isotope signal.

### Dissolved Stream Si Isotope Composition as a Tool to Monitor Future Hyporheic Zone Functioning

Given the consistency of the DSi concentrations, Ge/Si ratios and  $\delta^{30}\text{Si}_{\text{DSi}}$  compositions during three austral summers and our understanding of these Si isotopes compositions in Crescent Stream, we can assess the potential use of stream water  $\delta^{30}\text{Si}_{\text{DSi}}$  compositions to trace future changes in hyporheic zone functioning in response to predicted scenarios in McMurdo Dry Valleys (Doran et al., 2008; Fountain et al., 2014).

Increased air temperatures in Antarctica (Bekryaev et al., 2010) are driving increased glacial melting with subsequent impact on stream flow with exceptionally high flow events reported in 2001–2002, 2008–2009, and 2011–2012 (Doran et al., 2008). In this study, we observe no relationship between  $\delta^{30}\text{Si}_{\text{DSi}}$  values and stream flow in Crescent Stream between 2014 and 2017 suggesting that  $\delta^{30}\text{Si}_{\text{DSi}}$  values will not respond to increased stream water flow in the future. However, increases in stream flow and decreases in fluid transit time in MDV streams will likely move the hyporheic zone toward a weathering limited regime (Wlostowski et al., 2018) where secondary clay

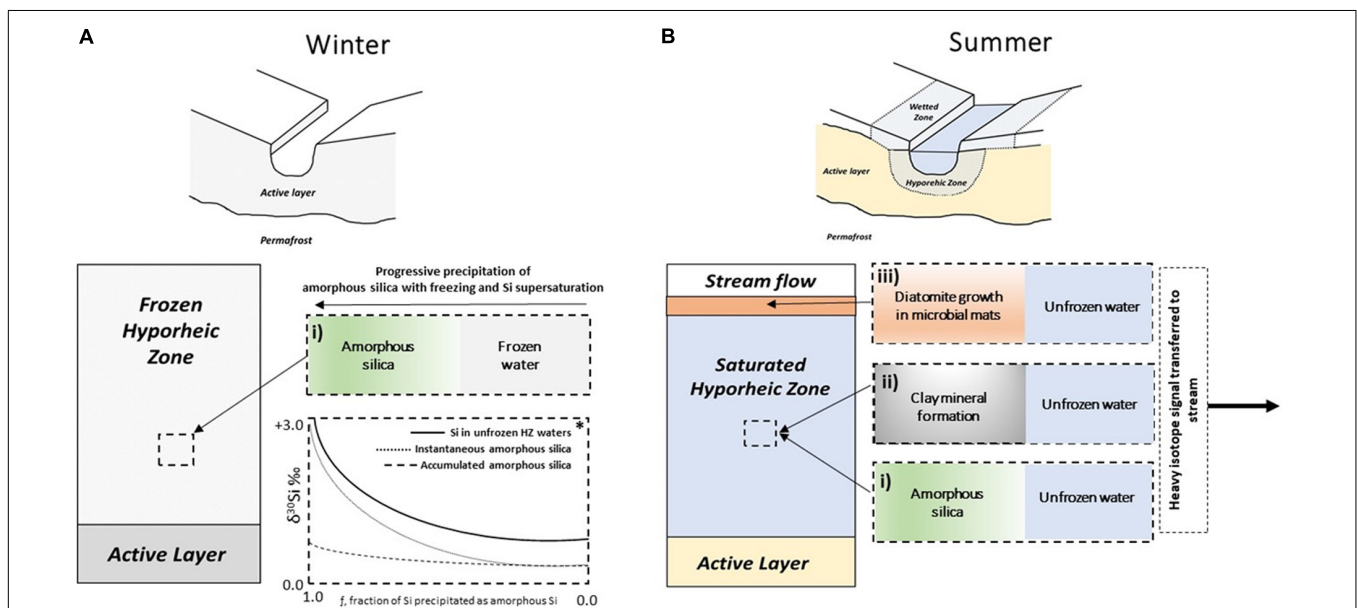


**FIGURE 9** | Schematic showing the principal processes controlling dissolved Si isotope compositions in Crescent Stream during the austral winter (**A**) and summer (**B**) months. The initial pool of  $\text{Si}(\text{OH})_4$  is supplied by primary mineral dissolution (Gooseff et al., 2002) in the hyporheic zone. Si isotope fractionation occurs during subsequent secondary inorganic and biologically mediated Si phases formation. During winter (**A**) waters in isolated pockets of the hyporheic zone freeze, resulting in supersaturation of  $\text{Si}(\text{OH})_4$  and precipitation of amorphous silica (i). Under these conditions, unidirectional kinetic isotope fractionation occurs in accordance with the Rayleigh fractionation model (\*) and amorphous silica preferentially incorporates the light isotopes ( $^{30}\epsilon = -1.0\text{‰}$ ), leaving the remaining unfrozen water with relatively high  $\delta^{30}\text{Si}$  compositions. With progressive amorphous silica formation, the Si isotope composition of  $\text{Si}(\text{OH})_4$  in unfrozen water evolves to heavier values. During summer (**B**), ice in the hyporheic zone thaws and the remaining DSi (in equilibrium with amorphous Si) presenting high  $\delta^{30}\text{Si}_{\text{DSi}}$  compositions is released from the isolated pockets into Crescent Stream. In addition, diatoms are actively forming in microbial mats (ii) in the hyporheic zone during summer months, preferentially taking up light Si isotopes, providing a background contribution of higher  $\delta^{30}\text{Si}_{\text{DSi}}$  compositions in Crescent Stream. These processes are superimposed onto clay mineral formation (iii), also preferentially taking up light Si isotopes.

minerals are dissolved and removed faster than they can be replaced via incongruent silicate mineral dissolution. This change in weathering regime may alter the  $\delta^{30}\text{Si}_{\text{DSi}}$  composition of waters in contact with clay minerals during summer months.

Soil and water temperatures are predicted to increase in MDV (Fountain et al., 2014). Under future conditions, saline waters may not reach the low temperatures required for cryogenic precipitates to form, leaving a larger pool of silicon unfrozen during winter months and altering the isotope composition of DSi released into Crescent Stream during the summer. One scenario might be that in earlier warming stages, more regular freeze-thaw cycles would promote higher proportions of amorphous silica precipitation and therefore enhance Si isotope fractionation towards heavier values in the residual solution (Dietzel, 2005). In later stages, increased soil temperatures and induced thaw are likely to connect hyporheic zone pockets. Under these conditions, amorphous silica precipitation would no longer occur in a closed system and the heavy  $\delta^{30}\text{Si}_{\text{DSi}}$  would not be preserved in the isolated pockets during the winter months.

Thermokarst erosion is also predicted to increase in MDV streams (Levy et al., 2013). In January 2012, thermokarst erosion in the west fork of Crescent Stream resulted in a brief (hours to days) increase in DSi concentrations (Gooseff et al., 2016), suggesting that more frequent thermokarst events may increase the supply of Si to streams. During these events, Si may be transported as particulate and colloidal amorphous silica and clay minerals and so contribute silicon with silicate rock to lower  $\delta^{30}\text{Si}_{\text{DSi}}$  values. Increased thermokarst may also lead to increased disturbance of the stream bed and transport of diatoms in particulate organic matter (McKnight et al., 1999; Cullis et al., 2014) as has been observed during the 2001–2002, 2008–2009, and 2011–2012 high flow seasons (Kohler et al., 2015). In this study water samples were filtered at 0.4  $\mu\text{m}$ . At this pore size, colloids can pass through 0.4  $\mu\text{m}$  filters and contribute to the dissolved Si concentration. In the future, the silicon concentrations and Si isotope compositions of separate particulate, colloidal and truly dissolved fractions would be required to fully capture variations in the supply of silicon to MDV streams in response to these erosion events.

## CONCLUSION

This study reports the first  $\delta^{30}\text{Si}_{\text{DSi}}$  isotope compositions and Ge/Si ratios of dissolved Si in Crescent Stream, Antarctica during three austral seasons between 2014 and 2017. The  $\delta^{30}\text{Si}_{\text{DSi}}$  isotope compositions and Si concentrations in Antarctica streams are higher than reported in northern latitude wet-based glaciers and form a narrow cluster within the values reported in permafrost-dominated Arctic rivers, evidence for a non-glacial silicate weathering in Antarctica.

The  $\delta^{30}\text{Si}_{\text{DSi}}$  compositions in Crescent Stream are higher than  $\delta^{30}\text{Si}$  compositions in silicate rocks showing that no direct weathering signal from primary mineral dissolution is transferred to the stream. Instead, the  $\delta^{30}\text{Si}_{\text{DSi}}$  and Ge/Si data highlight that biotic and abiotic interactions occur within the hyporheic zone and influence the dissolved silicon released to the

stream. Stream water-derived silicate mineral weathering rates in high latitudes are likely underestimated because a fraction of DSi is incorporated into secondary weathering products (i.e., clay minerals and amorphous silica) in the hyporheic zone. Amorphous silica precipitation within isolated pockets of hyporheic zone during winter months likely contributes to the stream  $\delta^{30}\text{Si}_{\text{DSi}}$  isotope compositions showing that a winter process can affect the summer-dissolved signal.

$\delta^{30}\text{Si}_{\text{DSi}}$  values, Ge/Si ratios and Si concentrations show no seasonal or diurnal variation because glacial meltwaters are in equilibrium with these secondary Si products on the water transit timescales of hours to days. The constant  $\delta^{30}\text{Si}_{\text{DSi}}$  compositions through the summer demonstrates a homogeneous functioning of the hyporheic zone, whether it is a near-stream zone or an extended zone.

The ongoing summer warming of the glacial surfaces of dry based glaciers and increased soil surface temperatures in McMurdo Dry Valleys is leading to increased glacial meltwater supply, changing hyporheic zone capacity and possible thermokarst erosion in streams. Here we show that Si isotopes are a useful tool to monitor possible shifts in the formation of secondary weathering products in the hyporheic zone of the McMurdo Dry Valley streams.

## DATA AVAILABILITY STATEMENT

All datasets generated for this study are included in the article/**Supplementary Material**.

## AUTHOR CONTRIBUTIONS

SO, CH, WB, and DM conceived the project. CH, FG, and SO analyzed the samples. All authors contributed to the discussion of data and manuscript writing.

## FUNDING

This project received funding from the European Union's Horizon 2020 research and innovation program under grant agreement Nos. 714617 and 678371. FG and SO acknowledge funding from the National Funds for Scientific Research FNRS (Grant Nos. 26043653 and FC69480). JH and KH acknowledge funding from the Royal Society Enhancement Award (Grant RGF\EA\181036). SW, DM, and WB acknowledge the NSF grant to the MCM LTER project OPP-ANT 1115249.

## ACKNOWLEDGMENTS

We would like to thank Anne Iserentant, Claudine Givron, Elodie Devos, and H el ene Dailly from the analytical platform MOCA at UCLouvain. The McMurdo Dry Valleys LTER team is acknowledged for their long-term collection of gauge data and sample collection during 2014–2017 field seasons at

Crescent Stream, MDV. We acknowledge Joshua Darling for the identification of diatom taxa in microbial mats in Crescent Stream. We also acknowledge the Subsurface Energy Materials Characterization and Analysis Laboratory (SEMCAL), School of Earth Sciences, The Ohio State University for SEM images.

## REFERENCES

- Abraham, K., Opfergelt, S., Fripiat, F., Cavagna, A.-J., de Jong, J., Foley, S. F., et al. (2008).  $\delta^{30}\text{Si}$  and  $\delta^{29}\text{Si}$  determinations on USGS BHVO-1 and BHVO-2 reference materials with a new configuration on a Nu Plasma Multi-Collector ICP-MS. *Geostand. Geoanal. Res.* 32, 193–202. doi: 10.1111/j.1751-908x.2008.00879.x
- Alger, A. S. (1997). *Ecological Processes in a Cold Desert Ecosystem: The Abundance and Species Distribution of Algal Mats in Glacial Meltwater Streams in Taylor Valley, Antarctica*. Boulder: University of Colorado.
- Alleman, L. Y., Cardinal, D., Cocquyt, C., Plisnier, P. D., Descy, J. P., Kimirei, I., et al. (2005). Silicon isotopic fractionation in Lake Tanganyika and its main tributaries. *J. Great Lakes Res.* 31, 509–519. doi: 10.1016/s0380-1330(05)70280-x
- Anderson, S. P., Drever, J. I., and Humphrey, N. F. (1997). Chemical weathering in glacial environments. *Geology* 25, 399–402.
- Armtyage, R. M. G., Georg, G. R. B., Savage, P. S., Williams, H. M., and Halliday, A. N. (2011). Silicon isotopes in meteorites and planetary core formation. *Geochim. Cosmochim. Acta* 75, 3662–3676. doi: 10.1016/j.gca.2011.03.044
- Bekryaev, R. V., Polyakov, I. V., Vladimir, A., and Alexeev, V. A. (2010). Role of polar amplification in long-term surface air temperature variations and modern Arctic warming. *J. Clim.* 23, 3888–3906. doi: 10.1175/2010jcli3297.1
- Berner, R. A., and Berner, E. K. (1997). “Silicate weathering and climate,” in *Tectonic Uplift and Climate Change*, ed. W. F. Ruddiman (Boston, MA: Springer), 353–365. doi: 10.1007/978-1-4615-5935-1\_15
- Bernstein, L. R. (1985). Germanium geochemistry and mineralogy. *Geochim. Cosmochim. Acta* 49, 2409–2422. doi: 10.1016/0016-7037(85)90241-8
- Biskaborn, B. K., Smith, S. L., Noetzi, J., Matthes, H., Vieira, G., Streletskiy, D. A., et al. (2019). Permafrost is warming at a global scale. *Nat. Commun.* 10:264.
- Bockheim, J. G. (2002). Landform and soil development in the McMurdo Dry Valleys, Antarctica: a regional synthesis. *Arctic Antarctic Alpine Res.* 34, 308–317. doi: 10.1080/15230430.2002.12003499
- Bockheim, J. G., Campbell, I. B., and McLeod, M. (2007). Permafrost distribution and active-layer depths in the McMurdo Dry Valleys, Antarctica. *Permafrost. Periglac. Process.* 18, 217–227. doi: 10.1002/ppp.588
- Brzezinski, M. A., Jones, J. L., Bidle, K. D., and Azam, F. (2003). The balance between silica production and silica dissolution in the sea: insights from Monterey Bay, California, applied to the global data set. *Limnol. Oceanogr.* 48, 1846–1854. doi: 10.4319/lo.2003.48.5.1846
- Burkins, M. B., Virginia, R. A., and Wall, D. H. (2001). Organic carbon cycling in Taylor Valley, Antarctica: quantifying soil reservoirs and soil respiration. *Glob. Change Biol.* 7, 113–125. doi: 10.1046/j.1365-2486.2001.00393.x
- Campbell, I. B., and Claridge, G. G. C. (1987). *Antarctica: Soils, Weathering Processes and Environment*, Vol. 16. Amsterdam: Elsevier.
- Cardinal, D., Alleman, L. Y., De Jong, J., Ziegler, K., and André, L. (2003). Isotopic composition of silicon measured by multicollector plasma source mass spectrometry in dry plasma mode. *J. Anal. Atom. Spectr.* 18, 213–218. doi: 10.1039/b210109b
- Channing, A., and Butler, I. B. (2007). Cryogenic opal-A deposition from Yellowstone hot springs. *Earth Planet. Sci. Lett.* 257, 121–131. doi: 10.1016/j.epsl.2007.02.026
- Conovitz, P. A. (2000). *Active Layer Dynamics and Hyporheic Zone Storage in Three Streams in the McMurdo Dry Valleys, Antarctica*. Doctoral dissertation, Colorado State University, Fort Collins.
- Conovitz, P. A., MacDonald, L. H., and McKnight, D. M. (2006). Spatial and temporal active layer dynamics along three glacial meltwater streams in the McMurdo Dry Valleys, Antarctica. *Arctic Antarctic Alpine Res.* 38, 42–53. doi: 10.1657/1523-0430(2006)038[0042:satald]2.0.co;2
- Conovitz, P. A., McKnight, D. M., MacDonald, L. H., and Fountain, A. G. (1998). *Fryxell Basin, Antarctica*, Vol. 72. Washington, DC: American Geophysical Union, 93.
- Cooper, A. F., Adam, L. J., Coulter, R. F., Eby, G. N., and McIntosh, W. C. (2007). Geology, geochronology and geochemistry of a basaltic volcano, White Island, Ross Sea, Antarctica. *J. Volcanol. Geother. Res.* 165, 189–216. doi: 10.1016/j.jvolgeores.2007.06.003
- Cornelis, J. T., Delvaux, B., Georg, R., Lucas, Y., Ranger, J., and Opfergelt, S. (2011). Tracing the origin of dissolved silicon transferred from various soil-plant systems towards rivers: a review. *Biogeosci. Discuss.* 8, 89–112. doi: 10.5194/bg-8-89-2011
- Cozzetto, K., McKnight, D. M., Nylén, T., and Fountain, A. (2006). Experimental investigations into processes controlling stream and hyporheic temperatures, Fryxell Basin, Antarctica. *Adv. Water Res.* 29, 130–153. doi: 10.1016/j.advwatres.2005.04.012
- Cozzetto, K. D., Bencala, K. E., Gooseff, M. N., and McKnight, D. M. (2013). The influence of stream thermal regimes and preferential flow paths on hyporheic exchange in a glacial meltwater stream. *Water Resour. Res.* 49, 5552–5569. doi: 10.1002/wrcr.20410
- Cullis, J. D., Stanish, L. F., and McKnight, D. M. (2014). Diel flow pulses drive particulate organic matter transport from microbial mats in a glacial meltwater stream in the McMurdo Dry Valleys. *Water Resour. Res.* 50, 86–97. doi: 10.1002/2013wr014061
- Darling, J. P., Garland, D. D., Stanish, L. F., Esposito, R. M., Sokol, E. R., and McKnight, D. M. (2017). Thermal autecology describes the occurrence patterns of four benthic diatoms in McMurdo Dry Valley streams. *Polar Biol.* 40, 2381–2396. doi: 10.1007/s00300-017-2151-y
- Delstanche, S., Opfergelt, S., Cardinal, D., Elsass, F., André, L., and Delvaux, B. (2009). Silicon isotopic fractionation during adsorption of aqueous monosilicic acid onto iron oxide. *Geochim. Cosmochim. Acta* 73, 923–934. doi: 10.1016/j.gca.2008.11.014
- Delvigne, C., Opfergelt, S., Cardinal, D., Delvaux, B., and André, L. (2009). Distinct silicon and germanium pathways in the soil-plant system: Evidence from banana and horsetail. *J. Geophys. Res.* 114:G02013. doi: 10.1029/2008JG000899
- Demarest, M. S., Brzezinski, M. A., and Beucher, C. P. (2009). Fractionation of silicon isotopes during biogenic silica dissolution. *Geochim. Cosmochim. Acta* 73, 5572–5583. doi: 10.1016/j.gca.2009.06.019
- Derry, L. A., Kurtz, A. C., Ziegler, K., and Chadwick, O. A. (2005). Biological control of terrestrial silica cycling and export fluxes to watersheds. *Nature* 433, 728–731. doi: 10.1038/nature03299
- Dietzel, M. (2005). Impact of cyclic freezing on precipitation of silica in Me–SiO<sub>2</sub>–H<sub>2</sub>O systems and geochemical implications for cryosols and sediments. *Chem. Geol.* 216, 79–88. doi: 10.1016/j.chemgeo.2004.11.003
- Doran, P. T., McKay, C. P., Fountain, A. G., Nylén, T., McKnight, D. M., Jaros, C., et al. (2008). Hydrologic response to extreme warm and cold summers in the McMurdo Dry Valleys, East Antarctica. *Antarctic Sci.* 20, 499–509. doi: 10.1017/s0954102008001272
- Doran, P. T., Priscu, J. C., Lyons, W. B., Walsh, J. E., Fountain, A. G., McKnight, D. M., et al. (2002). Antarctic climate cooling and terrestrial ecosystem response. *Nature* 415:517. doi: 10.1038/nature710
- Dowling, C. B., Lyons, W. B., and Welch, K. A. (2013). Strontium isotopic signatures of streams from Taylor Valley, Antarctica, revisited: the role of carbonate mineral dissolution. *Aquat. Geochem.* 19, 231–240. doi: 10.1007/s10498-013-9189-4
- Dowling, C. B., Welch, S. A., and Lyons, W. B. (2019). The geochemistry of glacial deposits in Taylor Valley, Antarctica: comparison to upper continental crustal abundances. *Appl. Geochem.* 107, 91–104. doi: 10.1016/j.apgeochem.2019.05.006
- Egan, K. E., Rickaby, R. E., Leng, M. J., Hendry, K. R., Hermoso, M., Sloane, H. J., et al. (2012). Diatom silicon isotopes as a proxy for silicic acid utilisation: a

## SUPPLEMENTARY MATERIAL

The Supplementary Material for this article can be found online at: <https://www.frontiersin.org/articles/10.3389/feart.2020.00229/full#supplementary-material>



- Southern Ocean core top calibration. *Geochim. Cosmochim. Acta* 96, 174–192. doi: 10.1016/j.gca.2012.08.002
- Esposito, R. M. M., Spaulding, S. A., McKnight, D. M., Van de Vijver, B. A. R. T., Kopalová, K., Lubinski, D., et al. (2008). Inland diatoms from the McMurdo Dry valleys and James Ross Island, Antarctica. *Botany* 86, 1378–1392. doi: 10.1139/b08-100
- Fernandez, N. M., Zhang, X., and Druhan, J. L. (2019). Silicon isotopic re-equilibration during amorphous silica precipitation and implications for isotopic signatures in geochemical proxies. *Geochim. Cosmochim. Acta* 262, 104–127. doi: 10.1016/j.gca.2019.07.029
- Fountain, A. G., Levy, J. S., Gooseff, M. N., and Van Horn, D. (2014). The McMurdo Dry Valleys: a landscape on the threshold of change. *Geomorphology* 225, 25–35. doi: 10.1016/j.geomorph.2014.03.044
- Frings, P. J., Clymans, W., Fontorbe, G., Christina, L., and Conley, D. J. (2016). The continental Si cycle and its impact on the ocean Si isotope budget. *Chem. Geol.* 425, 12–36. doi: 10.1016/j.chemgeo.2016.01.020
- Froelich, P. N., Blanc, V., Mortlock, R. A., Chillrud, S. N., Dunstan, W., Udomkit, A., et al. (1992). River fluxes of dissolved silica to the ocean were higher during glacial: Ge/Si in diatoms, rivers, and oceans. *Paleoceanography* 7, 739–767. doi: 10.1029/92pa02090
- Gaspard, F., Opfergelt, S., Amerijeiras-Marino, Y., Dessert, C., Derry, L., and Delmelle, P. (2019). “Si isotopes and Ge/Si ratios as weathering proxy in streams of Guadeloupe: methodological development and first results,” in *Symposium « Non-Traditional Stable Isotopes in Glacial and Non-Glacial Environments »*, 7<sup>th</sup> January 2019 (Louvain-la-Neuve: UCLouvain).
- Georg, R. B., Halliday, A. N., Schauble, E. A., and Reynolds, B. C. (2007b). Silicon in the Earth's core. *Nature* 447, 1102–1106.
- Georg, R. B., Reynolds, B. C., Frank, M., and Halliday, A. N. (2006). New sample preparation techniques for the determination of Si isotopic compositions using MC-ICP-MS. *Chem. Geol.* 235, 95–104. doi: 10.1016/j.chemgeo.2006.06.006
- Georg, R. B., Reynolds, B. C., West, A. J., Burton, K. W., and Halliday, A. N. (2007a). Silicon isotope variations accompanying basalt weathering in Iceland. *Earth Planet. Sci. Lett.* 261, 476–490. doi: 10.1016/j.epsl.2007.07.004
- Gooseff, M., and McKnight, D. (2019). *McMurdo Dry Valleys LTER: High Frequency Seasonal Stream Gage Measurements from Crescent Stream at F8 in Taylor Valley, Antarctica from 1990 to present. Environmental Data Initiative*. Available online at: <https://doi.org/10.6073/pasta/86bce67070a2e3b7bf5ca805059fee> (accessed June 1, 2020).
- Gooseff, M. N., McKnight, D. M., Lyons, W. B., and Blum, A. E. (2002). Weathering reactions and hyporheic exchange controls on stream water chemistry in a glacial meltwater stream in the McMurdo Dry Valleys. *Water Resour. Res.* 38, 15–11.
- Gooseff, M. N., McKnight, D. M., Runkel, R. L., and Vaughn, B. H. (2003). Determining long time-scale hyporheic zone flow paths in Antarctic streams. *Hydrol. Process.* 17, 1691–1710. doi: 10.1002/hyp.1210
- Gooseff, M. N., Van Horn, D., Sudman, Z., McKnight, D. M., Welch, K. A., and Lyons, W. B. (2016). Stream biogeochemical and suspended sediment responses to permafrost degradation in stream banks in Taylor Valley, Antarctica. *Biogeosciences* 13, 1723–1732. doi: 10.5194/bg-13-1723-2016
- Hall, B. L., Denton, G. H., and Hendy, C. H. (2000). Evidence from Taylor Valley for a grounded ice sheet in the Ross Sea, Antarctica. *Geografiska Annaler Ser. A Phys. Geogr.* 82, 275–303. doi: 10.1111/1468-0459.00126
- Hatton, J. E., Hendry, K. R., Hawkings, J. R., Wadham, J. L., Kohler, T. J., Stibal, M., et al. (2019). Investigation of subglacial weathering under the Greenland Ice Sheet using silicon isotopes. *Geochim. Cosmochim. Acta* 247, 191–206. doi: 10.1016/j.gca.2018.12.033
- Hatton, J. E., Hendry, K. R., Hawkings, J. R., Wadham, J. L., Opfergelt, S., Kohler, T. J., et al. (2019). Silicon isotopes in Arctic and sub-Arctic glacial meltwaters: the role of subglacial weathering in the silicon cycle. *Proc. R. Soc. A* 475, 20190098. doi: 10.1098/rspa.2019.0098
- Howard-Williams, C., Vincent, C. L., Broady, P. A., and Vincent, W. F. (1986). Antarctic stream ecosystems: variability in environmental properties and algal community structure. *Int. Rev. Gesamten Hydrobiol. Hydrogr.* 71, 511–544. doi: 10.1002/iroh.19860710405
- Kohler, T. J., Stanish, L. F., Crisp, S. W., Koch, J. C., Liptzin, D., Baeseman, J. L., et al. (2015). Life in the main channel: long-term hydrologic control of microbial mat abundance in McMurdo Dry Valley streams, Antarctica. *Ecosystems* 18, 310–327. doi: 10.1007/s10021-014-9829-6
- Kurtz, A. C., Derry, L. A., and Chadwick, O. A. (2002). Germanium-silicon fractionation in the weathering environment. *Geochim. Cosmochim. Acta* 66, 1525–1537. doi: 10.1016/s0016-7037(01)00869-9
- Levy, J. S., Fountain, A. G., Dickson, J. L., Head, J. W., Okal, M., Marchant, D. R., et al. (2013). Accelerated thermokarst formation in the McMurdo Dry Valleys, Antarctica. *Sci. Rep.* 3, 1–8.
- Li, Y., Tiping, D., and Defang, W. (1995). Experimental study of silicon isotope dynamic fractionation and its application in geology. *Chin. J. Geochem.* 14, 212–219. doi: 10.1007/bf02842044
- Lyons, W., and Welch, K. (2015). McMurdo Dry Valleys LTER: stream chemistry and ion concentrations. *Environ. Data Initiat.* doi: 10.6073/pasta/be9f781814330116f68844a8957962e4
- Lyons, W. B., Nezat, C. A., Benson, L. V., Bullen, T. D., Graham, E. Y., Kidd, J., et al. (2002). Strontium isotopic signatures of the streams and lakes of Taylor Valley, Southern Victoria Land, Antarctica: chemical weathering in a polar climate. *Aquat. Geochem.* 8, 75–95.
- Lyons, W. B., Welch, K. A., Fountain, A. G., Dana, G. L., Vaughn, B. H., and McKnight, D. M. (2003). Surface glaciochemistry of Taylor Valley, southern Victoria Land, Antarctica and its relationship to stream chemistry. *Hydrol. Process.* 17, 115–130. doi: 10.1002/hyp.1205
- Lyons, W. B., Welch, K. A., Neumann, K., Toxey, J. K., Mearthar, R., Williams, C., et al. (1998). Geochemical linkages among glaciers, streams and lakes within the Taylor Valley, Antarctica. *Antarctic Res. Ser.* 72, 77–92. doi: 10.1029/ar072p0077
- Maurice, P. A., McKnight, D. M., Leff, L., Fulghum, J. E., and Gooseff, M. (2002). Direct observations of aluminosilicate weathering in the hyporheic zone of an Antarctic Dry Valley stream. *Geochim. Cosmochim. Acta* 66, 1335–1347. doi: 10.1016/s0016-7037(01)00890-0
- Mavromatis, V., Rinder, T., Prokushkin, A. S., Pokrovsky, O. S., Korets, M. A., Chmeleff, J., et al. (2016). The effect of permafrost, vegetation, and lithology on Mg and Si isotope composition of the Yenisey River and its tributaries at the end of the spring flood. *Geochim. Cosmochim. Acta* 191, 32–46. doi: 10.1016/j.gca.2016.07.003
- McKnight, D. M., Alger, A. S., Tate, C. M., Shupe, G., and Spaulding, S. (1998). “Longitudinal patterns in algal abundance and species distribution in meltwater streams in Taylor Valley, Southern Victoria Land, Antarctica,” in *Ecosystem Dynamics in a Polar Desert: The McMurdo Dry Valleys, Antarctica: Antarctic Research Series*, Vol. 73, ed. J. C. Prisco (Washington, DC: American Geophysical Union), 109–128.
- McKnight, D. M., Niyogi, D. K., Alger, A. S., Bomblies, A., Conovitz, P. A., and Tate, C. M. (1999). Dry Valley streams in Antarctica: ecosystems waiting for water. *BioScience* 49, 985–995.
- McKnight, D. M., Runkel, R. L., Duff, J. H., Tate, C. M., and Moorhead, D. (2004). Inorganic nitrogen and phosphorous dynamics of Antarctic glacial meltwater streams as controlled by hyporheic exchange and benthic autotrophic communities. *J. N. Am. Benthol. Soc.* 23, 171–188. doi: 10.1899/0887-3593(2004)023<0171:inapdo>2.0.co;2
- McKnight, D. M., and Tate, C. M. (1997). Canada stream: a glacial meltwater stream in Taylor Valley, south Victoria Land, Antarctica. *J. N. Am. Benthol. Soc.* 16, 14–17. doi: 10.2307/1468224
- McKnight, D. M., Tate, C. M., Andrews, E. D., Niyogi, D. K., Cozzetto, K., Welch, K., et al. (2007). Reactivation of a cryptobiotic stream ecosystem in the McMurdo Dry Valleys, Antarctica: a long-term geomorphological experiment. *Geomorphology* 89, 186–204. doi: 10.1016/j.geomorph.2006.07.025
- Mortlock, R. A., and Froelich, P. N. (1996). Determination of germanium by isotope dilution-hydride generation inductively coupled plasma mass spectrometry. *Anal. Chim. Acta* 332, 277–284. doi: 10.1016/0003-2670(96)00230-9
- Mullin, J., and Riley, J. P. (1955). The colorimetric determination of silicate with special reference to sea and natural waters. *Anal. Chim. Acta* 12, 162–176. doi: 10.1016/s0003-2670(00)87825-3
- Murnane, R. J., and Stallard, R. F. (1990). Germanium and silicon in rivers of the Orinoco drainage basin. *Nature* 344, 749–752. doi: 10.1038/344749a0
- Nezat, C. A., Lyons, W. B., and Welch, K. A. (2001). Chemical weathering in streams of a polar desert (Taylor Valley, Antarctica). *Geol. Soc. Am. Bull.* 113, 1401–1408. doi: 10.1130/0016-7606(2001)113<1401:cwisoa>2.0.co;2

- Obu, J., Westermann, S., Vieira, G., Abramov, A., Balks, M., Bartsch, A., et al. (2020). Pan-Antarctic map of near-surface permafrost temperatures at 1 km2 scale. *Cryosphere* 14, 497–519. doi: 10.5194/tc-14-497-2020
- Oelze, M., Von Blanckenburg, F., Bouchez, J., Hoellen, D., and Dietzel, M. (2015). The effect of Al on Si isotope fractionation investigated by silica precipitation experiments. *Chem. Geol.* 397, 94–105. doi: 10.1016/j.chemgeo.2015.01.002
- Oelze, M., von Blanckenburg, F., Hoellen, D., Dietzel, M., and Bouchez, J. (2014). Si stable isotope fractionation during adsorption and the competition between kinetic and equilibrium isotope fractionation: Implications for weathering systems. *Chem. Geol.* 380, 161–171. doi: 10.1016/j.chemgeo.2014.04.027
- Opfergelt, S., Bournonville, G., Cardinal, D., André, D., Delstanche, S., and Delvaux, B. (2009). Impact of soil weathering degree on silicon isotopic fractionation during adsorption onto iron oxides in basaltic ash soils, Cameroon. *Geochim. Cosmochim. Acta* 73, 7226–7240. doi: 10.1016/j.gca.2009.09.003
- Opfergelt, S., and Delmelle, P. (2012). Silicon isotopes and continental weathering processes: Assessing controls on Si transfer to the ocean. *Comptes Rend. Geosci.* 344, 723–738. doi: 10.1016/j.crte.2012.09.006
- Opfergelt, S., Delvaux, B., André, L., and Cardinal, D. (2008). Plant silicon isotopic signature might reflect soil weathering degree. *Biogeochemistry* 91, 163–175. doi: 10.1007/s10533-008-9278-4
- Opfergelt, S., Eiriksdottir, E. S., Burton, K. W., Einarsson, A., Siebert, C., Gislason, S. R., et al. (2011). Quantifying the impact of freshwater diatom productivity on silicon isotopes and silicon fluxes: Lake Myvatn, Iceland. *Earth Planet. Sci. Lett.* 305, 73–82. doi: 10.1016/j.epsl.2011.02.043
- Opfergelt, S., Williams, H. M., Cornelis, J.-T., Guicharnaud, R. A., Georg, R. B., Siebert, C., et al. (2017). Iron and silicon isotope behaviour accompanying weathering in Icelandic soils, and the implications for iron export from peatlands. *Geochim. Cosmochim. Acta* 217, 273–291. doi: 10.1016/j.gca.2017.08.033
- Pokrovski, G. S., and Schott, J. (1998). Experimental study of the complexation of silicon and germanium with aqueous organic species: implications for germanium and silicon transport and Ge/Si ratio in natural waters. *Geochim. Cosmochim. Acta* 62, 3413–3428. doi: 10.1016/s0016-7037(98)00249-x
- Pokrovski, O. S., Reynolds, B. C., Prokushkin, A. S., Schott, J., and Viers, J. (2013). Silicon isotope variations in Central Siberian rivers during basalt weathering in permafrost-dominated larch forests. *Chem. Geol.* 355, 103–116. doi: 10.1016/j.chemgeo.2013.07.016
- Pretorius, W., Weis, D., Williams, G., Hanano, D., Kieffer, B., and Scoates, J. (2006). Complete trace elemental characterisation of granitoid (USGS G–2, GSP–2) reference materials by high resolution inductively coupled plasma–mass spectrometry. *Geostand. Geoanal. Res.* 30, 39–54. doi: 10.1111/j.1751-908x.2006.tb00910.x
- Pugh, H. E., Welch, K. A., Lyons, W. B., Priscu, J. C., and McKnight, D. M. (2002). The biogeochemistry of Si in the McMurdo Dry Valley lakes, Antarctica. *Int. J. Astrobiol.* 1, 401–413. doi: 10.1017/s1473550403001332
- Reynolds, B. C., Aggarwal, J., André, L., Baxter, D., Beucher, C., Brzezinski, M. A., et al. (2007). An inter-laboratory comparison of Si isotope reference materials. *J. Anal. Atomic Spectrometry* 22, 561–568.
- Savage, P. S., Georg, R. B., Armytage, R. M. G., Williams, H. M., and Halliday, A. N. (2010). Silicon isotope homogeneity in the mantle. *Earth Planet. Sci. Lett.* 295, 139–146. doi: 10.1016/j.epsl.2010.03.035
- Savage, P. S., Georg, R. B., Williams, H. M., Burton, K. W., and Halliday, A. N. (2011). Silicon isotope fractionation during magmatic differentiation. *Geochim. Cosmochim. Acta* 75, 6124–6139. doi: 10.1016/j.gca.2011.07.043
- Scribner, A. M., Kurtz, A. C., and Chadwick, O. A. (2006). Germanium sequestration by soil: targeting the roles of secondary clays and Fe-oxyhydroxides. *Earth Planet. Sci. Lett.* 243, 760–770. doi: 10.1016/j.epsl.2006.01.051
- Spaulding, S., Esposito, R., Lubinski, D., Horn, S., Cox, M., McKnight, D., et al. (2020). *Antarctic Freshwater Diatoms Website*. Available online at: <http://huey.colorado.edu/diatoms/about/index.php> (accessed June 9, 2020)
- Stanish, L. F., Nemergut, D. R., and McKnight, D. M. (2011). Hydrologic processes influence diatom community composition in Dry Valley streams. *J. N. Am. Benthol. Soc.* 30, 1057–1073. doi: 10.1899/11-008.1
- Sun, X., Möhr, C. M., Porcelli, D., Kutscher, L., Hirst, C., Murphy, M. J., et al. (2018). Stable silicon isotopic compositions of the Lena River and its tributaries: implications for silicon delivery to the Arctic Ocean. *Geochim. Cosmochim. Acta* 241, 120–133. doi: 10.1016/j.gca.2018.08.044
- Sutton, J., Ellwood, M. J., Maher, W. A., and Croot, P. L. (2010). Oceanic distribution of inorganic germanium relative to silicon: germanium discrimination by diatoms. *Glob. Biogeochem. Cycles* 24, 1–13. doi: 10.1029/2009GB003689
- Wetzel, F., De Souza, G. F., and Reynolds, B. C. (2014). What controls silicon isotope fractionation during dissolution of diatom opal? *Geochim. Cosmochim. Acta* 131, 128–137. doi: 10.1016/j.gca.2014.01.028
- Witherow, R. A., Lyons, W. B., and Henderson, G. M. (2010). Lithium isotopic composition of the McMurdo Dry Valleys aquatic systems. *Chem. Geol.* 275, 139–147. doi: 10.1016/j.chemgeo.2010.04.017
- Wlostowski, A. N., Gooseff, M. N., McKnight, D. M., and Lyons, W. B. (2018). Transit times and rapid chemical equilibrium explain chemostasis in glacial meltwater streams in the McMurdo Dry Valleys, Antarctica. *Geophys. Res. Lett.* 45, 13–322.
- Yeghicheyan, D., Carignan, J., Valladon, M., Le Coz, M. B., Cornec, F. L., Castrec–Rouelle, M., et al. (2001). A compilation of silicon and thirty one trace elements measured in the natural river water reference material SLRS–4 (NRC–CNRC). *Geostand. Newsl.* 25, 465–474. doi: 10.1111/j.1751-908x.2001.tb00617.x
- Young, E. D., Galy, A., and Nagahara, H. (2002). Kinetic and equilibrium mass-dependent isotope fractionation laws in nature and their geochemical and cosmochemical significance. *Geochim. Cosmochim. Acta* 66, 1095–1104. doi: 10.1016/s0016-7037(01)00832-8
- Ziegler, K., Chadwick, O. A., Brzezinski, M. A., and Kelly, E. F. (2005). Natural variations of  $\delta^{30}\text{Si}$  ratios during progressive basalt weathering, Hawaiian Islands. *Geochim. Cosmochim. Acta* 69, 4597–4610. doi: 10.1016/j.gca.2005.05.008

**Conflict of Interest:** The authors declare that the research was conducted in the absence of any commercial or financial relationships that could be construed as a potential conflict of interest.

Copyright © 2020 Hirst, Opfergelt, Gaspard, Hendry, Hatton, Welch, McKnight and Berry Lyons. This is an open-access article distributed under the terms of the Creative Commons Attribution License (CC BY). The use, distribution or reproduction in other forums is permitted, provided the original author(s) and the copyright owner(s) are credited and that the original publication in this journal is cited, in accordance with accepted academic practice. No use, distribution or reproduction is permitted which does not comply with these terms.